

석사학위논문

CRLH 전송선로를 이용한
고조파 제어 마이크로파 F급
전력증폭기

2019 년 8 월 22 일

전 북 대 학 교 대 학 원

전 자 정 보 공 학 부

Phanam Pech

CRLH 전송선로를 이용한
고조파 제어 마이크로파 F급
전력증폭기

Microwave Class-F Power Amplifier Using Harmonic
Control CRLH Transmission Lines

2019 년 8 월 22 일

전 북 대 학 교 대 학 원

전 자 정 보 공 학 부

Phanam Pech

CRLH 전송선로를 이용한
고조파 제어 마이크로파 F급
전력증폭기

지도교수 정용채

이 논문을 공학 석사 학위논문으로 제출함.

2019 년 4 월 23 일

전 북 대 학 교 대 학 원

전 자 정 보 공 학 부

Phanam Pech

Phanam Pech 의 석사학위논문을 인준함.

위 원 장 전북대학교 교 수 임동구 (인)

부위원장 전북대학교 교 수 김정무 (인)

위 원 전북대학교 교 수 정용채 (인)

2019 년 6 월 20 일

전 북 대 학 교 대 학 원

Contents

List of Figures	iii
List of Acronyms	v
Abstract	vi
Chapter 1 Introduction.....	1
1.1 Literature review	1
1.2 Dissertation Objective and Organization	2
Chapter 2 Power Amplifier.....	4
2.1 Basic of Power Amplifier	4
2.1.1 Amplifier Gain and efficeincy.....	4
2.1.2 Amplifier classification	6
2.1.3 High Efficiency Power Amplifier.....	8
2.2 Class-F Power Amplifier	9
Chapter 3 Composite Right-/Left-Handed Transmission Line	14
3.1 Right-Handed and Left-Handed Transmission Lines	14
3.2 CRLH TLs	16
3.3 Balanced CRLH TL and Dual-Band Property	18
Chapter 4 Class-F PA using Harmonic Control CRLH TLs.....	26
4.1 Harmonic Control Circuit using CRLH TL	26
4.1.1 Bias circuit using CRLH TL	26
4.1.2 Analysis of an Unbalance and Asymmetric CRLH TL Biasing Cicuit.....	28
4.1.3 Analysis of an Impedance Transformer using CRLH TL	36

4.2 Class-F Power Amplifier Design	39
4.2.1 Load-pull Method.....	39
4.2.2 Bias Circuit Design	40
4.2.3 Harmonic Impedance Transformer.....	43
4.2.4 Matching Network Design	45
4.2.5 Simulation Results.....	48
Chapter 5 Conclusions and Future Work.....	51
References	52
Abstract in Korean	54

List of Figures

Figure 2.1 Fourier analysis of reduced conduction angle current waveform.	6
Figure 2.2 RF power (relate to class A) and effeciency as a function of conduction agle.....	7
Figure 2.3 Schematic of class-F power amplifier.	9
Figure 2.4 A class-F power amplifier ideal topology with ideal current and voltage waveforms.....	11
Figure 2.5 Harmonic control network for class-F PAs.	13
Figure 2.6 Input impedance obtained by harmonic control network for class-F PAs	13
Figure 3.1 RH-TL structure.	14
Figure 3.2 LH-TL structure.	15
Figure 3.3 The phase resoponse of RH-TL and LH-TL.	16
Figure 3.4 Equivalent circuit model for ideal CRLH TL	17
Figure 3.5 Graphic representation of the dispersion equation for CRLH TL.	19
Figure 3.6 Balance CRLH TL in T-type structure	20
Figure 3.7 Balance CRLH TL in Pi-type structure	21
Figure 3.8 Simulation result od Pi-type balance structure.....	25
Figure 4.1 Unbalance and asymmetrical CRLH TL	27
Figure 4.2 Unbalance and asymmetric CRLH bias circuit.....	27
Figure 4.3 The equivalent circuit of bias circuit.....	28

Figure 4.4 The structure of impedance transformer circuit	36
Figure 4.5 The procedure to obtain the impedance to output matching network.....	38
Figure 4.6 PAE and power deliver to the load contours from load-pull simulation	40
Figure 4.7 Bias circuit with harmonic control using CRLH TL.....	41
Figure 4.8 Simulation performance of proposed bias circuit	42
Figure 4.9 Harmonic impedance transforming structure.....	43
Figure 4.10 Simulation performances of harmonic impedance transformer	44
Figure 4.11 PAs design and impedance matching	45
Figure 4.12 The equivalent circuit of class-F PA with harmonic control using CRLH TLs	46
Figure 4.13 Input matching network with stability and bias circuits	47
Figure 4.14 Harmonic control circuit and output matching network	47
Figure 4.15 <i>S</i> -parameters of class-F PA	48
Figure 4.16 Gain, drain efficiency and PAE along the output power	49
Figure 4.17 Stability factor of the designed class-F PA	49
Figure 4.18 Output power, gain, and drain efficiency along the frequencies.....	50

List of Acronyms

CRLH	Composite right-/left-handed
DE	Drain efficiency
HCC	Harmonic control circuit
IMN	Input matching network
LH-TL	Left-handed transmission line
MSL	Microstrip line
N	Number of unit cell
OMN	Output matching network
PA	Power amplifier
PAE	Power added efficiency
PCS	Personal communication system
RH-TL	Right-handed transmission line
RZ	Reflection zero
TZ	Transmission zero
Z_L	Load impedance
Z_s	Source impedance
λ	Wavelength
Γ	Reflection coefficient

ABSTRACT

Microwave Class-F Power Amplifier Using Harmonics Control CRLH Transmission Lines

Phanam Pech

Division of Electronics and Information Engineering

The Graduate School

Chonbuk National University

This dissertation presents the analysis of unbalance and asymmetric composite right-/left-handed transmission line (CRLH TL) can control up to third harmonic frequency for class-F power amplifier (PA). This CRLH TL is applied into biasing circuit design with the harmonic control purpose. The length of the TL in the proposed biasing circuit is smaller than a quarter wavelength ($\lambda/4$). Instead of using $\lambda/4$ TL, the impedance transformer is also analyzed with CRLH TL to obtain short and open circuit for $2f_0$ and $3f_0$ at the drain terminal of the transistor, respectively. As a result, the proposed impedance transformer circuit can complete the requirement with the electrical length of the TL less than 90° .

Proposed microwave class-F PA using harmonic control CRLH TL was designed and simulated at 1.96 GHz for personal communication services (PCS) application. The proposed PA achieved output power and drain efficiency of 13.61 W, 70.39%, respectively in non-ideal simulation.

Keywords: CRLH TL, Harmonic, PA, PCS.

Chapter 1 Introduction

1.1 Literature Review

With the advancement of wireless communication systems, power amplifiers (PAs) with high efficiency is becoming more and more important as they consume small power of the system and closely relate to the thermal dissipation. Extensive research has been devoted to improving the efficiency of PAs through enhancement in all design methods. Finding materials sustaining higher operating voltages, e.g., GaN, developing device structures with higher breakdown voltage, e.g., LDMOS transistor and fashioning circuit techniques to reduce power dissipation in the transistor, e.g., harmonic control, are the example of the efforts made to improve the efficiency of PAs [1].

In base station (BS) applications, power consumption is one of the most critical requirements, which requires that the PAs used must have a high gain to amplify the weak signal and a high power added efficiency (PAE), regardless of whether the required PAs are working in a single band or multiple bands concurrently. In order to improve the PAEs of the PAs, switched-mode or harmonic-tuned PAs have been paid much consideration and especially the class-F, as well as the inverse class-F (F^{-1}) are being adopted widely [2], [3]. However, the harmonic tuning circuits, such as those used in class-F amplifiers, could increase the size and cost of the PAs which are already complicated with the sophisticated architectures, unless effective measures are taken to miniaturize and simplify the circuit. The researchers

have been used composite right-/left-handed (CRLH) transmission line (TL) to reduce the size of the harmonic tuning circuit. Even though the small size of harmonic tuning circuit but, the DC-biasing circuits using quarter wavelength microstrip line (MSL) stub occupies in a large area, creates difficulties for miniaturization of the overall amplifier circuit. Recently, a novel DC-biasing circuit with harmonic control for compact high efficiency power amplifiers have demonstrated by using CRLH TL . Despite the size of the biasing circuit is reduced but a quarter wavelength impedance transformer transmission line is needed to control the harmonics for class-F PA and there is no analysis of the structure. In this dissertation, a microwave class-F PA is designed with harmonics control using CRLH TL to obtain high efficiency and the mathematical analysis of the proposed structures are presented.

1.2 Dissertation Objective and Organization

The main objective of this dissertation is to design a microwave class-F power amplifier using harmonics control CRLH TL for PCS downlink communication system. Firstly, the CRLH TL stub operate as a bias circuit with harmonics control is investigated. This bias circuit with 2 unit cells CRLH TL can control the fundamental frequency (open circuit), the second and third harmonics (short circuit) different from the bias circuit designed with quarter wavelength transmission line. Secondly, the CRLH TL operates as the harmonic impedance transformer to provide short and open circuit at the drain terminal of the transistor to satisfy class-F PA condition.

This dissertation is organized as below. Chapter 1 introduces shortly about PAs and some of its applications. Chapter 2 covers fundamental of PAs design,

classification, efficiency and harmonic control PAs. Chapter 3 introduce the CRLH TL and its advantages in microwave circuit design. Chapter 4 describe class-F PA design method, CRLH TL operates as the bias circuit and harmonic impedance transformer TL. The analysis and simulation are presented in this chapter.

Finally, Chapter 5 summarize the fundamental, design goal that contributed to this dissertation and future work.

Chapter 2 Power Amplifier

In this chapter, the fundamental of the power amplifier and high efficiency power amplifier are presented.

2.1 Fundamental of Power Amplifier

The amplifier is an electronic device used to increase the magnitude of voltage, current, power of an input signal. It takes in a weak electrical signal or waveform and reproduces a similar stronger waveform at the output by using an external power source. Depending on changes it makes to the input signal, amplifiers are broadly classified into current, voltage and power amplifiers.

A power amplifier is an electronic amplifier designed to increase the magnitude of the power of a given input signal. RF and microwave PAs are devices that amplify the input RF signal and deliver greater power at the output. PA can also be considered as a device that converts DC power provided from the supply into RF power at the output.

PAs are used in many different applications including the majority of wireless and radio communication systems, wireless and cable TV broadcast system, optical driver amplifier, audio systems, and radars.

2.1.1 Gain and Efficiency

One of the many important parameters of an amplifier is its gain. The gain of an amplifier can be described as voltage gain, current gain, and power gain. The power amplifier is generally defined as its power gain.

$$G = P_{out} - P_{in} \quad (2.1)$$

Another important parameter is power conversion efficiency. Power conversion efficiency is a measure of how effectively an amplifier converts power drawn from the external source (DC-supply) to useful RF signal power delivered to the load. Most popular efficiencies in power amplifier are drain efficiency (η) and power added efficiency (PAE) with units in percentage (%).

$$\eta = \frac{P_{Out}}{P_{DC}} \quad (2.2)$$

$$\text{PAE} = \frac{P_{Out} - P_{in}}{P_{DC}} \quad (2.3)$$

Where, P_{in} , P_{out} and P_{DC} are RF input, RF output power and the DC-power from DC-supply to the drain circuit of power amplifier, respectively.

The power that is not converted to useful signal power is dissipated as heat. As a result, the efficiency of PA is reduced according to power dissipation.

Power amplifiers are normally designed for operation over a specific frequency or bandwidth. The transmitter band has a gain is almost constant over this bandwidth. Outside of the transmitter band or passband, the gain response tends to drop off at both lower and higher frequencies.

2.1.2 Amplifier Classification

The class of operation is referred to as the output waveform when an input signal is applied or more specifically, the transistor conduction angle has very important for power amplifiers in terms of linearity and efficiency. In any given design there is always a trade-off between linearity and efficiency, as linearity increases, efficiency decreases and efficiency increase as linearity decreases. There are many types of power amplifiers and they differ from each other in terms of their linearity, efficiency, and output power capability. To design a power amplifier we have to understand the design factor and choose the amplifier operation type most suited for the target application. Depending on the linearity and efficiency requirements, the operation classes of the amplifier can be divided into two groups. The first

group is for high linearity application such as class A, B, and AB. The second group belongs to high efficiency but low linearity such as class C, D, E, F, inverse class F, J, etc.

The conduction angle is defined as the proportion of the RF cycle during which the transistor is conducting.

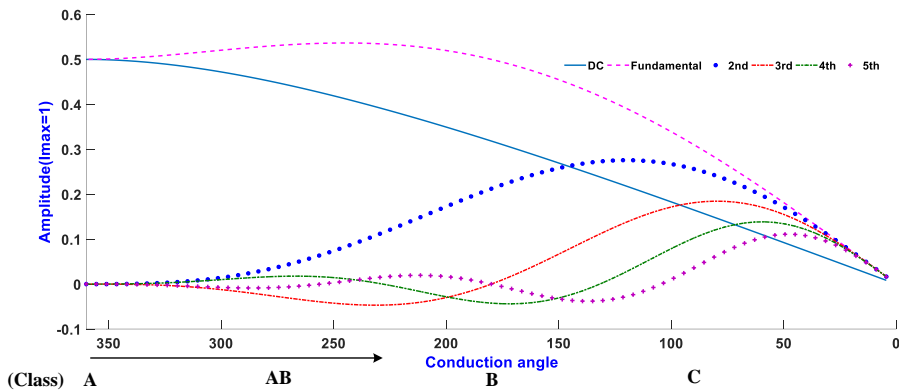


Fig. 2.1. Fourier analysis of reduced conduction angle current waveform.

Fig. 2.1 shows the current waveform of different conduction angles (α) for class A, B, AB, and C. The second up to fifth harmonics are plotted. At class AB range up to the middle of class B, the second harmonic is also presented with the fundamental. The conduction angle of drain current is reduced by lowering the gate bias point. Besides this, the input voltage cycle drops below the threshold voltage and prevent the transistor from conducting current. Fig. 2.2 shows the RF power and efficiency as a function of conduction angles for optimum load and harmonics are assumed short. Between class A and class B operation, the fundamental RF output power is approximately constant, showing a few tenths dB increase in the mid-AB range over the class A output power. The class B condition delivers the same power as class A, but with a DC supply reduced by a factor of $\pi/2$ compared to class A, giving an ideal efficiency of $\pi/4$. The class C condition shows an increasing efficiency as the conduction angle is reduced to a low value, this is, however, accompanied by a substantial reduction in RF output power [4].

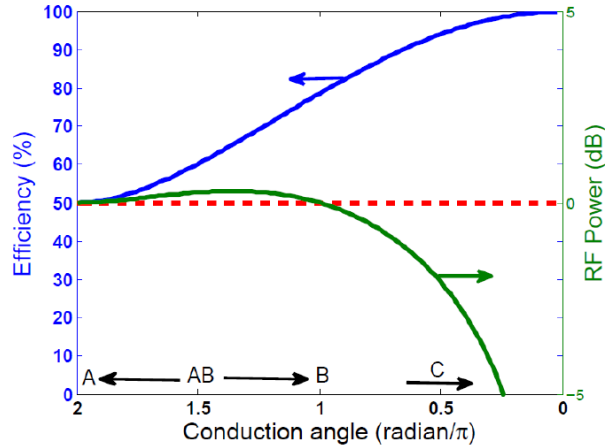


Fig. 2.2. RF power (relative to class A) and efficiency as a function of conduction angle (optimum load and harmonic short assumed).

2.1.3 High Efficiency Power amplifier

High efficiency is a crucial design consideration not only for the power amplifier (PA) itself but also for the transmitters. Several PA topologies, such as class-E, class-F, and inverse class-F (F^{-1}), have been proposed to achieve high efficiencies. In the class-E PA, a transistor acts as a switch. The voltage of the class-E amplifier is generated by charging and discharging of the output capacitor in parallel with the switch. Since this amplifier tunes all harmonic components using the LC resonator, it delivers the highest efficiency among the proposed amplifiers. However, the charging step of the capacitor cannot be abrupt. The capacitor cannot discharge fast enough to support the ideal waveform when operates at very high frequency. As a result, the efficiency of class-E PA is degraded significantly at high frequency.

To deliver high efficiency at high frequency, the harmonically tuned PAs, such as class-F and class- F^{-1} , have been extensively studied. The ideal class-F power amplifier has half-sinusoidal current and rectangular voltage

waveforms in conjunction with the short circuit for even harmonics and open circuit for odd harmonics. Thus, there is no overlapping between the current and voltage, resulting in approximately zero internal dissipation power. In addition, since there is no harmonic power, the class-F amplifier delivers the efficiency of approximately 100%.

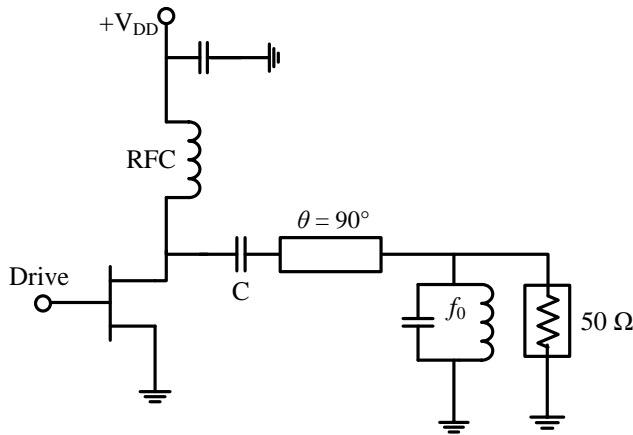


Fig. 2.3. Schematic of class-F power amplifier.

The class-F⁻¹ is a dual of the class-F PA where the current and voltage waveforms are interchanged. With the same drain supply voltage, the class-F⁻¹ has a larger peak voltage value than that of class-F, incurring the reliability problem due to the breakdown of the device. Thus, some research has compared and analyzed the class-F and class-F⁻¹ PAs under the condition of the same voltage swing. Due to advances in wide bandgap semiconductor technology such as gallium-nitride (GaN) high electron-mobility transistor (HEMT) technology, a large voltage swing becomes feasible and the obstacles in PA design are reduced.

2.2 Class-F Power Amplifier

High-power consumption mainly occurs due to the low efficiency of the power amplifier, where a large portion of the DC-supply is converted into heat. This requires the cost with large spacing for cooling of the system. The power consumption causes degradation of the device performance such as the battery lifetime. The class-F power amplifier can be used to improve the power added efficiency (PAE) at low power levels, which uses an output filter to control the harmonic content of the drain voltage or the current waveforms, which shapes them to reduce the power dissipation by the transistor and to increase the efficiency. The active device is assumed as an ideal device switch. Therefore, the power amplifier achieves only a limited degree of compression, so that a relatively small number of harmonic is generated at the drain output. Even though the transistor acts as an ideal switch device for some part of the duty cycle, it spends a considerable transition time between the switching states, where this time is limited by the harmonic composition of the drain waveforms.

The class-F power amplifier is characterized by a square waveform for the drain voltage and a half-sinusoid waveform for the drain current. The class-F response is achieved when the harmonic control circuit provides a short circuit for the even harmonics and open circuit for the odd harmonics. This technique can obtain a theoretical 100% drain efficiency using wave shaping the drain voltage and current waveforms.

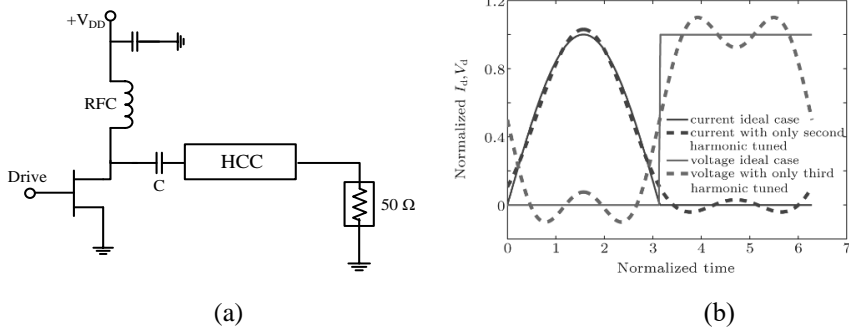


Fig. 2.4. (a) A class-F power amplifier ideal topology and (b) ideal current and voltage waveforms.

Therefore, it is widely used to increase the efficiency of PAs due to its simplicity and high performance. The harmonic control circuit (HCC) is an essential part of the design class-F PA, which can be implemented by the lumped or distributed elements. All the harmonic control circuits, which use the lumped and distributed elements, lead to the increment of the circuit size and complexity of the design procedure. Additionally, the use of the microstrip structures as a harmonic control circuit is widely used in the design. On the other hand, the tuning procedure is too complicated to adjust the structure at the desired frequency.

Fig. 2.4 (a) and (b) shows the simplified schematic of the class-F power amplifier, the drain current, and voltage, respectively. The current has the fundamental (first harmonic) and even harmonics, while the voltage has the fundamental and odd harmonics. Therefore, the harmonic control circuit should provide open circuit at odd harmonics and short circuit at even harmonics. In order to have effective control over the harmonics in the drain voltage and the drain current waveform, it is necessary to employ one of the several compact filters at the output port of the PA as suitable loads (short or

open) for the different harmonics. In this case, the current and voltage waveforms never overlap on each other and the dissipation of harmonic power may be eliminated. Therefore, the improvement of efficiency is expected.

$$I_d = i_{d,peak} \left(\frac{1}{\pi} + \frac{1}{2} \sin \omega_0 t - \frac{2}{\pi} \sum_{n=2,4,6,\dots}^{\infty} \frac{1}{n^2-1} \cos n\omega_0 t \right) \quad (2.4)$$

$$V_d = v_{d,peak} \left(\frac{1}{2} - \frac{2}{\pi} \sin \omega_0 t - \frac{2}{\pi} \sum_{n=3,5,7,\dots}^{\infty} \frac{1}{n} \sin n\omega_0 t \right) \quad (2.5)$$

Fig. 2.5 and Fig. 2.6 show a good example to understand harmonic control for class-F PAs [5]. The network is composed of two shunt stubs which control the second and third harmonic components. The transmission line elements, TL2 and TL3, are short and open circuit in order to provide terminating effect for even and odd harmonics, respectively. The physical length of TL2 and TL3 are $\lambda/4$ and $\lambda/12$ at the fundamental frequencies so it is equal to $\lambda/2$ and $\lambda/4$ at second and third harmonic frequencies. Then the input impedance at the connection point of TL1, TL2, and TL3 are shorted. These short impedances, 2S and 3S, are preserved constantly independent of the connected fundamental matching network (M/N). These both short impedances, 2S and 3S, are terminated to TL1 with the physical length of $\lambda/4$ at f_0 . The input impedance (Z_{in}) seen by the output stage of PAs is transformed into short (2S) and open (3O) impedances for the second and third harmonic frequencies, respectively.

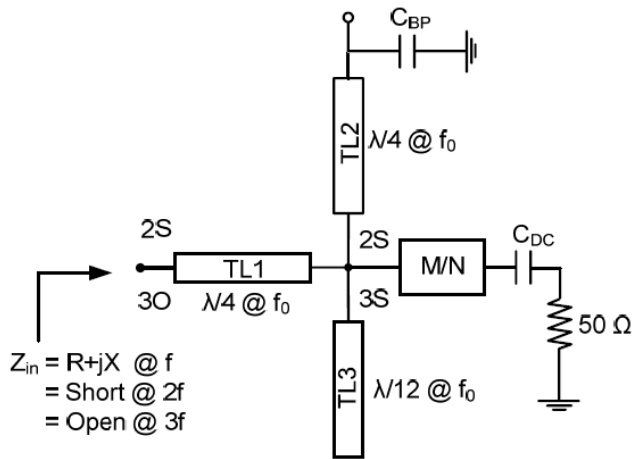


Fig. 2.5. Harmonic control network for class-F PAs.

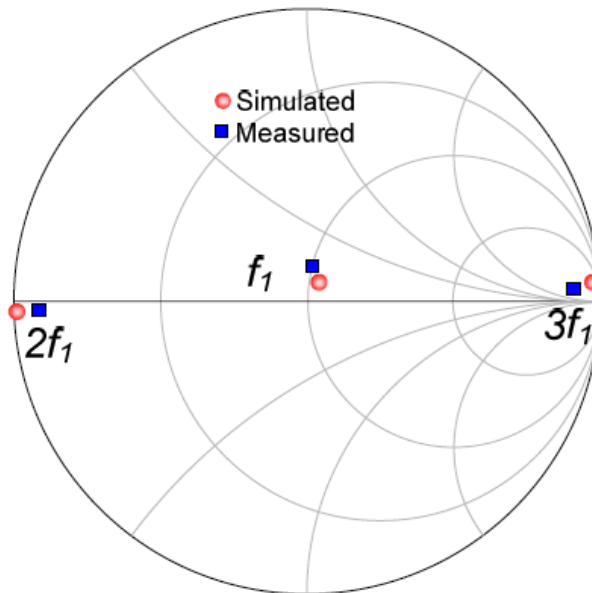


Fig. 2.6. Input impedance obtained by harmonic control network for class-F PAs.

Chapter 3 Composite Right-/Left-Handed (CRLH)

Transmission Line

3.1 Right-Handed and Left-Handed Transmission Line

The conventional transmission line (RH-TL) is represented by a series inductor and a shunt capacitor, implying the use of a low pass topology. By interchanging the position of the inductor and capacitor, the resulting structure is referred to as a left-handed transmission line (LH-TL) with a high pass configuration. The homogeneous models of a purely RH-TL and purely LH-TL are shown in Fig. 3.1 and Fig. 3.2. In the LH-TL, the phase and group velocities are composite to each other. Composite right-/left-handed (CRLH-TL) represent practical LH-TL because RH-TL parasitic effects are unavoidable when the realization of a LH-TL is attempt [6]-[8].

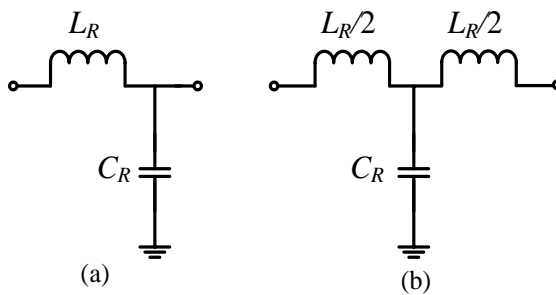


Fig. 3.1. RH-TL: (a) Asymmetric structure and (b) symmetric structure.

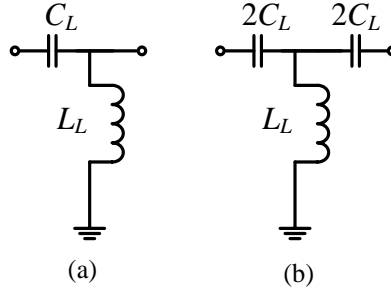


Fig. 3.2. LH-TL: (a) Asymmetric structure and (b) symmetric structure.

In these circuits, L_R , C_R and L_L , C_L are the distributed inductance and capacitance for RH-TL and LH-TL, respectively. For these equivalent circuits, the propagation constant and the characteristic impedance can be determined with the following formulas:

$$\gamma = \sqrt{Z'(\omega)Y'(\omega)} = \alpha + j\beta \quad (3.1)$$

$$Z_C = \sqrt{\frac{Z'(\omega)}{Y'(\omega)}} \quad (3.2)$$

Where $Z'(\omega)$ and $Y'(\omega)$ are the impedance of the series branch and the admittance of the parallel branch, α is the attenuation constant and β is the phase constant.

If the line is lossless ($\alpha = 0$), then the propagation constant is purely imaginary and the impedance is purely real. For RH-TL in Fig. 2.1 we can write:

$$Z'(\omega) = j\omega L_R', \quad Y'(\omega) = j\omega C_R' \quad (3.3a,b)$$

$$\beta = \omega\sqrt{L_R'C_R'} > 0, \quad Z_C = \sqrt{\frac{L_R'}{C_R'}} \quad (3.3c,d)$$

For LH-TL in Fig. 2.2 we can write:

$$Z'(\omega) = \frac{1}{j\omega C_L'}, \quad Y'(\omega) = \frac{1}{j\omega L_L'} \quad (3.4a,b)$$

$$\beta = -\frac{1}{\omega\sqrt{L_L' C_L'}} < 0, \quad Z_c = \sqrt{\frac{L_L'}{C_L'}} \quad (3.4c,d)$$

We consider the phase constant in equation (3.3c) and (3.4c). These equations are the dispersion equation for RH-TL and LH-TL, respectively. The phase response representation by these equations is given in Fig. 3.3.

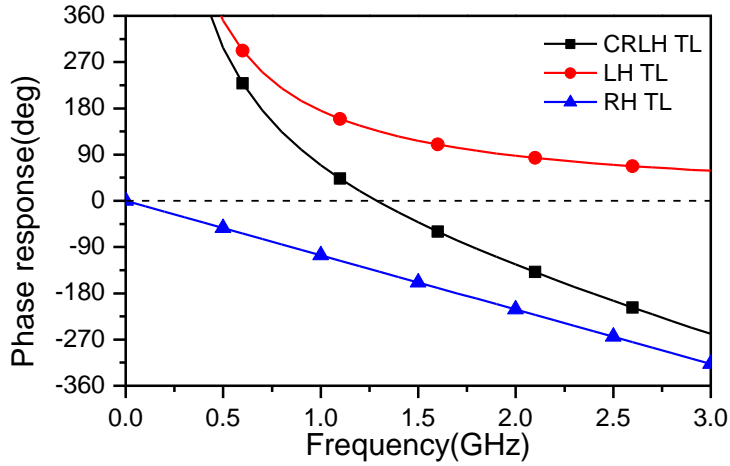


Fig. 3.3. The phase responses of RH-TL and LH-TL.

From the dispersion equations (3.3c) and (3.4c), the phase velocity can be obtained as, $v_p = \omega/\beta$ is positive for RH-TL and negative for LH-TL. The group velocity, $v_g = 1/(d\beta/d\omega)$, is positive for both RH-TL and LH-TL. Therefore, the energy is transported from generator to the load in both cases. Due to the negative phase velocity of LH-TL, the wave is propagated backward from load to generator.

3.2 CRLH TLs

The equivalent circuit of CRLH-TL is a combination of the RH-TL and LH-TL equivalent circuits. Fig. 3.4 shows the equivalent circuit of CRLH-TL, where, it is similar to RH-TL and LH-TL. It consists of a per-unit-length impedance Z' (Ω/m) constitute by a RH per-unit-length inductance L'_R (H/m) in series with a LH times-unit-length capacitance C'_L (F.m) and a per-unit-length admittance Y' (S/m) constituted by a RH per-unit-length capacitance C'_R (F/m) in parallel with a LH time-unit-length inductance L'_L (H.m).

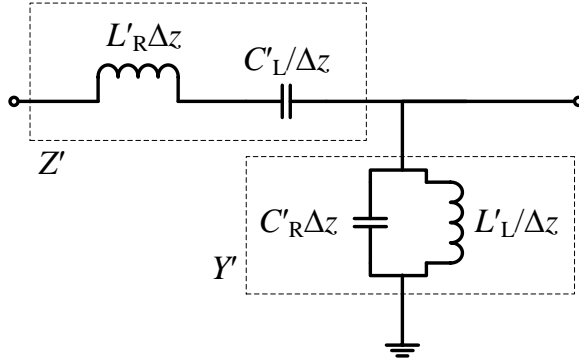


Fig. 3.4. Equivalent circuit model for the ideal CRLH TL.

Through Fig. 3.4 the equivalent impedance and admittance of CRLH-TL can be determined as:

$$Z' = j \left(\omega L'_R - \frac{1}{\omega C'_L} \right) \quad (3.5a)$$

$$Y' = j \left(\omega C'_R - \frac{1}{\omega L'_L} \right) \quad (3.5b)$$

Using (3.5a) and (3.5b) with the relations to (3.1) considered as a lossless circuit, we can obtain:

$$\gamma = \sqrt{ZY'} = 0 + j\beta$$

$$\begin{aligned} \Rightarrow \beta &= \frac{\sqrt{ZY'}}{j} \\ &= \frac{j \sqrt{\left(\omega L'_R - \frac{1}{\omega C'_L}\right) \left(\omega C'_R - \frac{1}{\omega L'_L}\right)}}{j} \\ &= \begin{cases} -\sqrt{\left(\omega L'_R - \frac{1}{\omega C'_L}\right) \left(\omega C'_R - \frac{1}{\omega L'_L}\right)} < 0, \text{ for } \omega < \omega_{sh}, \omega_{se} = 1/\sqrt{L'_R C'_L} & (3.6a) \\ +\sqrt{\left(\omega L'_R - \frac{1}{\omega C'_L}\right) \left(\omega C'_R - \frac{1}{\omega L'_L}\right)} > 0, \text{ for } \omega > \omega_{se}, \omega_{sh} = 1/\sqrt{L'_L C'_R} & (3.6b) \end{cases} \end{aligned}$$

where ω_{se} is the resonance frequency determined by the series combination of L'_R and C'_L and ω_{sh} is the resonance frequency determined by the shunt combination of L'_L and C'_R . For $\omega_{se} < \omega < \omega_{sh}$ the phase constant, β , is an imaginary number, therefore the propagation constant γ , is a real number, which means that the signal on the line is attenuated. Therefore, for $\omega_{se} < \omega < \omega_{sh}$, the circuit obtain a band-stop filter characteristic. If $\omega_{se} = \omega_{sh}$ then there is no stop-band. The circuit that can obtain $\omega_{se} = \omega_{sh} = \omega_0$ is called a balanced circuit and if not, then it is an unbalanced circuit.

We can design a balanced CRLH TL circuit, $\omega_{se} = \omega_{sh} = \omega_0$, when:

$$L'_R C'_L = L'_L C'_R \quad (3.7a)$$

$$Z_{RH} = Z_{LH} = \sqrt{\frac{L'_R}{C'_R}} = \sqrt{\frac{L'_L}{C'_L}} \quad (3.7b)$$

$$\omega_0 = \frac{1}{\sqrt{L'_R C'_L}} = \frac{1}{\sqrt{L'_L C'_R}} \quad (3.7c)$$

The characteristic impedance of CRLH TL in an unbalance case is obtained by substitute (3.5a) and (3.5b) into (3.2).

$$Z_{CRLH} = \sqrt{\frac{Z'}{Y'}} = \sqrt{\frac{L'_L}{C'_L}} \sqrt{\frac{\omega^2 L'_R C'_L - 1}{\omega^2 L'_L C'_R - 1}} \quad (3.8)$$

In a balanced case, the impedance of CRLH-TL can be determined by (3.7b). This means that $Z_{CRLH} = Z_{RH} = Z_{LH}$ and the impedance matching over a large frequency domain can be easily matched in a balanced case.

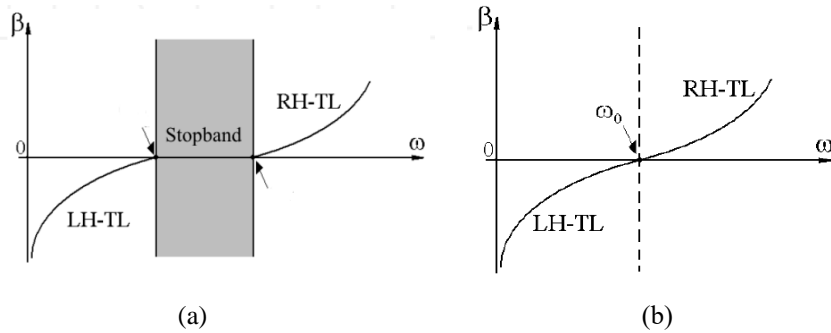


Fig. 3.5. Graphic representation of the dispersion equations for CRLH TL:

(a) unbalance case and (b) balance case.

For the balanced case, used the same methodes to calculate phase constant β as mentioned above, then we can determine β_{CRLH} as following:

$$\beta_{CRLH} = \frac{\omega^2 L'_R C'_L - 1}{\sqrt{L'_L C'_L}} = \omega \sqrt{L'_R C'_R} - \frac{1}{\omega \sqrt{L'_L C'_L}} = \beta_{RH} + \beta_{LH} \quad (3.9)$$

As a result, the equivalent circuit for a balanced CRLH-TL can be increased the number of the unit cell (N) by connecting in cascade the equivalent circuits of RH-TL and LH-TL.

3.3 Balanced CRLH TL and Dual-Band Property

Balanced CRLH TL is most popular in dual-band application. The merit of CRLH TL is not only dual-band property but also can reduce the size of the circuit. Fig. 3.6 shows the balanced circuit of CRLH TL combination as a T-type network.

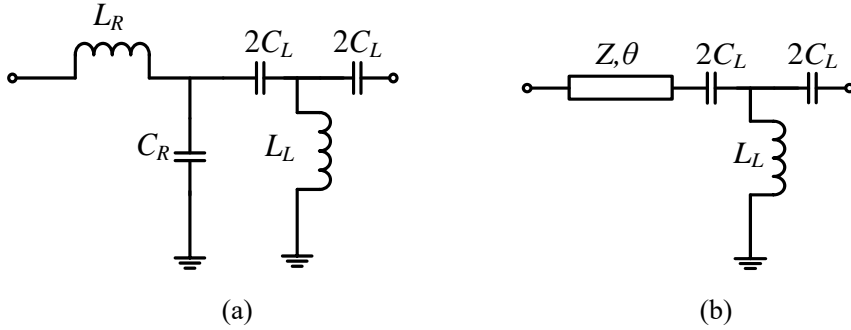


Fig. 3.6. Balanced CRLH TL: (a) Lumped element structure and (b) equivalent circuit with transmission line model.

In many works with the application of CRLH TL, the balance structure with C -first type combination of LH component is used and analyzed. In this chapter, we consider the balance CRLH TL with L -first type combination of LH component that it may be useful for the application that needs this kind of structure. The balanced CRLH TL with L -first type is constructed as a Pi-type network and it can obtain the same characteristic to balance CRLH TL with C -first type in T-type network model. The way to analyze this structure can be done as following.

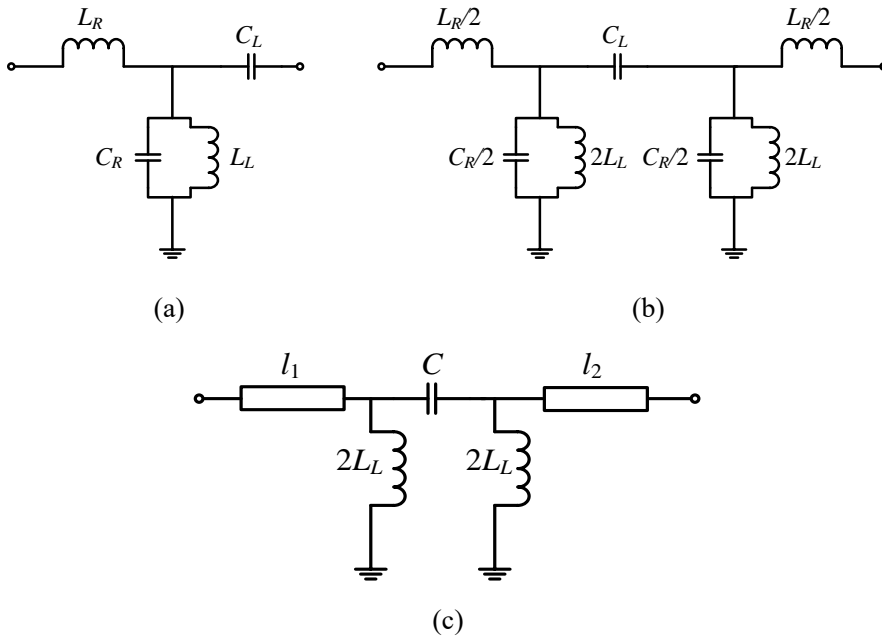


Fig. 3.7. Balanced L -first type CRLH TL: (a) Asymmetric structure, (b) symmetric structure, and (c) equivalent circuit of (b) in Pi-type model.

At first, we consider the ABCD parameters of the LH component.

$$\begin{aligned}
\begin{pmatrix} A & B \\ C & D \end{pmatrix}_{LH} &= \begin{pmatrix} 1 & 0 \\ \frac{1}{j2\omega L} & 1 \end{pmatrix} \begin{pmatrix} 1 & \frac{1}{j\omega C} \\ 0 & 1 \end{pmatrix} \begin{pmatrix} 1 & 0 \\ \frac{1}{j2\omega L} & 1 \end{pmatrix} \\
&= \begin{pmatrix} 1 & \frac{1}{j\omega C} \\ \frac{1}{j2\omega L} & -\frac{1}{2\omega^2 LC} + 1 \end{pmatrix} \begin{pmatrix} 1 & 0 \\ \frac{1}{j2\omega L} & 1 \end{pmatrix} \\
&= \begin{pmatrix} 1 - \frac{1}{2\omega^2 LC} & \frac{1}{j\omega C} \\ \frac{1}{j2\omega L} - \frac{1}{j4\omega^3 L^2 C} + \frac{1}{j2\omega L} & -\frac{1}{2\omega^2 LC} + 1 \end{pmatrix} \\
&= \begin{pmatrix} 1 - \frac{1}{2\omega^2 LC} & \frac{1}{j\omega C} \\ \frac{1}{j\omega L} - \frac{1}{j4\omega^3 L^2 C} & -\frac{1}{2\omega^2 LC} + 1 \end{pmatrix}
\end{aligned}$$

We can determine the phase response of the LH material through it

S-parameter (S_{21}).

$$\begin{aligned}
S_{21,LH} &= \frac{2}{A + B/Z_0 + CZ_0 + D} \\
&= \frac{2}{1 - \frac{1}{2\omega^2 LC} + \frac{1}{Z_0} \cdot \frac{1}{j\omega C} + Z_0 \left(\frac{1}{j\omega L} - \frac{1}{j4\omega^3 L^2 C} \right) - \frac{1}{2\omega^2 LC} + 1} \\
&= \frac{2}{2 - \frac{1}{\omega^2 LC} + \frac{1}{Z_0} \cdot \frac{1}{j\omega C} + Z_0 \left(\frac{1}{j\omega L} - \frac{1}{j4\omega^3 L^2 C} \right)} \\
\Rightarrow \phi_{LH} &= \tan^{-1} \left(\frac{\frac{1}{Z_0 \omega C} + \frac{Z_0}{\omega L} - \frac{Z_0}{4\omega^3 L^2 C}}{2 - \frac{1}{\omega^2 LC}} \right) = \tan^{-1} \left(\frac{\frac{1}{Z_0 \omega C} + \frac{Z_0}{4\omega L} \left(4 - \frac{1}{\omega^2 LC} \right)}{2 - \frac{1}{\omega^2 LC}} \right)
\end{aligned}$$

We can determine the overall phase of balanced CRLH TL as the combination of RH and LH phase responses.

$$\phi_{CRLH} = \phi_{RH} + \phi_{LH} = -\omega\sqrt{L_R C_R} + \tan^{-1} \left(\frac{\frac{1}{Z_0 \omega C_L} + \frac{Z_0}{4\omega L_L} \left(4 - \frac{1}{\omega^2 L_L C_L} \right)}{2 - \frac{1}{\omega^2 L_L C_L}} \right)$$

If $\omega_{LH} = \frac{1}{\sqrt{L_L C_L}}$, so

$$\phi_{LH} = \tan^{-1} \left(\frac{\frac{1}{Z_0 \omega C_L} + \frac{Z_0}{4\omega L_L} \left(4 - \left(\frac{\omega_{LH}}{\omega} \right)^2 \right)}{2 - \left(\frac{\omega_{LH}}{\omega} \right)^2} \right)$$

Assume: $\omega \gg \omega_{LH}$, $Z_0 = \sqrt{\frac{L_L}{C_L}}$ and

$$\tan^{-1} \left(\frac{\frac{1}{Z_0 \omega C_L} + \frac{Z_0}{4\omega L_L} \left(4 - \left(\frac{\omega_{LH}}{\omega} \right)^2 \right)}{2 - \left(\frac{\omega_{LH}}{\omega} \right)^2} \right) \approx \frac{\frac{1}{Z_0 \omega C_L} + \frac{Z_0}{4\omega L_L} \left(4 - \left(\frac{\omega_{LH}}{\omega} \right)^2 \right)}{2 - \left(\frac{\omega_{LH}}{\omega} \right)^2}$$

$$\Rightarrow \phi_{LH} \approx \frac{1}{2} \left(\frac{1}{Z_0 \omega C_L} + \frac{Z_0}{\omega L_L} \right)$$

$$\Rightarrow \phi_{LH} \approx \frac{1}{\omega \sqrt{L_L C_L}}$$

$$\phi_{CRLH} \approx -\omega\sqrt{L_R C_R} + \frac{1}{\omega \sqrt{L_L C_L}}$$

$$\phi_{CRLH} \approx -N\omega\sqrt{L_R C_R} + \frac{N}{\omega \sqrt{L_L C_L}} \quad (3.10)$$

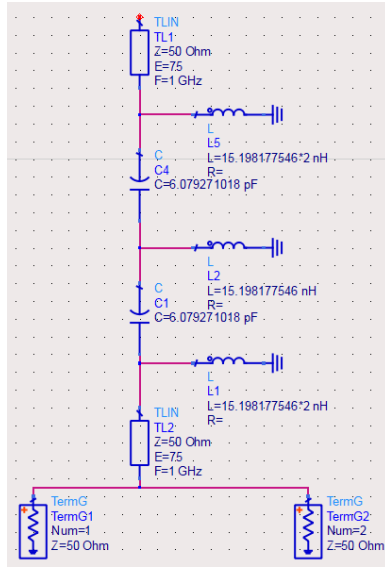
Through equation (3.10) we can consider the dual-band property of balanced CRLH with L -first in Pi-type structure as below.

$$-N\omega_1\sqrt{L_R C_R} + \frac{N}{\omega_1\sqrt{L_L C_L}} \approx \phi_1 \quad (3.11a)$$

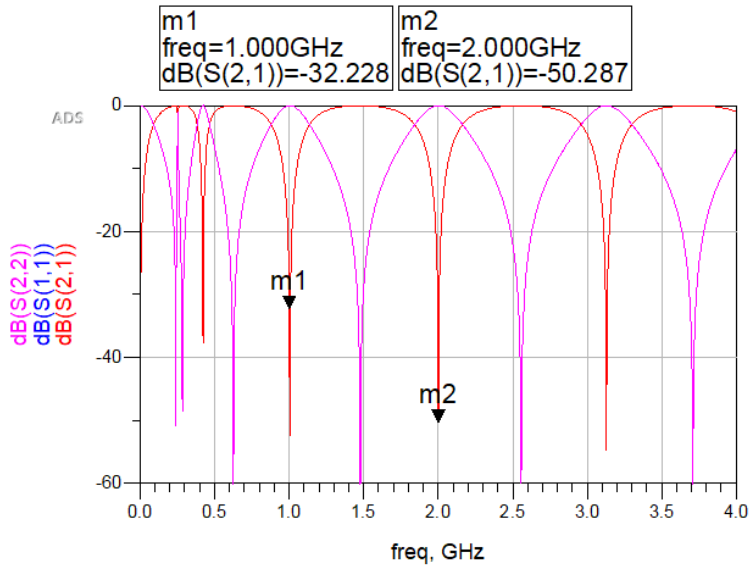
$$-N\omega_2\sqrt{L_R C_R} + \frac{N}{\omega_2\sqrt{L_L C_L}} \approx \phi_2 \quad (3.11b)$$

where N and ϕ are the number of the unit cell and phase of CRLH TL. Fig. 3.8 shows the simulation results to confirm the characteristic of this Pi-type balanced structure. The method to calculate the value of L_R , C_R , L_L , and C_L is already provided in [7] for T-type balance structure and we can also apply to Pi-type balance structure.

The simulation results in Fig. 3.8 is obtained from a Pi-type balance structure with $N=2$, $f_1=1\text{GHz}$, $f_2=2\text{GHz}$, and the phase difference between ϕ_1 and ϕ_2 is 180° . When this structure operates as a stub, it will provide two transmission zeros (TZs) at these mentioned frequencies.



(a)



(b)

Fig. 3.8. Pi-type balanced CRLH TL: (a) simulated circuit and (b) S-parameters.

Chapter 4 Class-F PA using Harmonic Control

CRLH TL

This chapter demonstrates the class-F PA with harmonic control circuit using CRLH TL. The analysis and simulation results are presented to prove the proposed idea.

4.1 Harmonic control circuit using CRLH TL

As mentioned in chapter 2, class-F power amplifier require short circuit at even harmonics and open circuit at odd harmonics to the drain of the transistor. In here, the bias circuit using CRLH TL operate as a quarter wavelength TL to control the second and third harmonics component and also reduce the size of the bias circuit.

4.1.1 Bias Circuit using CRLH TL

In chapter 3, the structure and characteristic of CRLH TL are already described. In designing a CRLH TL stub for bias circuit, L -first type structure is only one possible choice. The combination of this structure is RH-TL followed by shunt inductor and series of the capacitor. It is possible to feed the DC from the shunt inductor. In order to design a bias circuit with the ability to control the harmonic frequencies, in this work, we use the unbalanced and asymmetric structure of CRLH TL [9]-[12]. Fig. 4.1a shows the unbalanced and asymmetric CRLH TL structure with $N = 2$ where the first unit cell of LH is constructed by L_1 followed by series C_1 and the second unit cell is constructed by C_2 followed by shunt L_2 . As a result, we can obtain the equivalent circuit as Fig. 4.1b and the number of the lumped elements are

reduced.

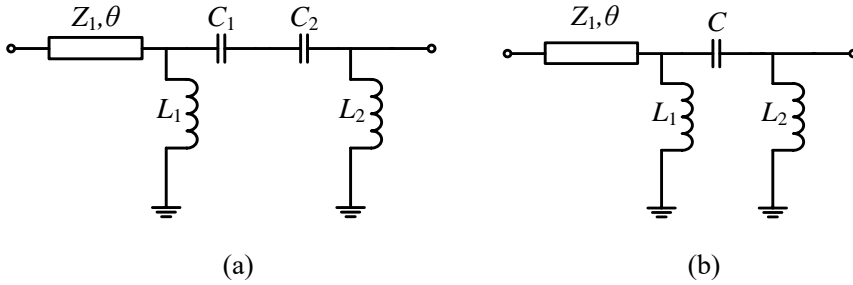


Fig. 4.1. Unbalanced and asymmetric CRLH TL: (a) 2 unit cells structure and (b) the equivalent circuit of (a).

The structure in Fig. 4.1b is preferable for biasing circuit design. When we use this structure to design a biasing circuit, it will operate as a one-port network (open-ended at port 2). The important thing is, it must provide an open circuit for fundamental frequency (f_0), the short circuit for the second ($2f_0$) and third ($3f_0$) harmonic frequencies at the connection point as shown in Fig. 4.2.

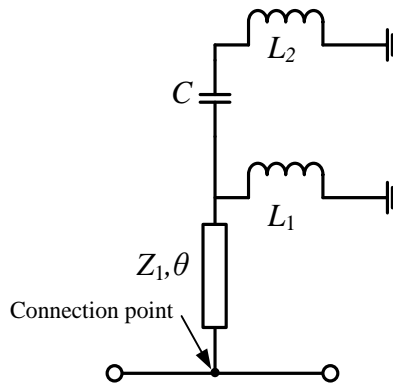


Fig. 4.2. Unbalance and asymmetric CRLH TL biasing circuit.

4.1.2 Analysis of an Unbalance CRLH TL Biasing Circuit

To obtain open circuit for fundamental (f_0) and short circuit for the second ($2f_0$) and third ($3f_0$) harmonic frequencies at the connection point of the circuit in Fig. 4.2, the impedance at this point is considered. Fig. 4.3 show the equivalent circuit of the bias circuit for our analysis. We can analyze this structure like the following.

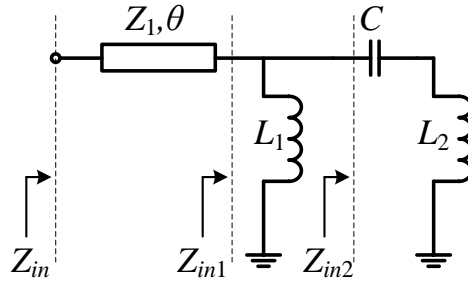


Fig. 4.3. The equivalent circuit of the biasing circuit.

- Determine for Z_{in2} :

$$\begin{aligned} Z_{in2} &= j\omega L_2 - j\frac{1}{\omega C} \\ &= j\left(\omega L_2 - \frac{1}{\omega C}\right) \end{aligned}$$

- Determine for Z_{in1} :

$$\begin{aligned} Z_{in1} &= \frac{j\omega L_1 \times Z_{in2}}{j\omega L_1 + Z_{in2}} = \frac{j\omega L_1 \times j\left(\omega L_2 - \frac{1}{\omega C}\right)}{j\omega L_1 + j\left(\omega L_2 - \frac{1}{\omega C}\right)} \\ &= j\frac{\omega L_1(\omega^2 L_2 C - 1)}{\omega^2 L_1 C + \omega^2 L_2 C - 1} \end{aligned}$$

➤ Determine for Z_{in} :

$$\begin{aligned}
 Z_{in} &= Z_1 \frac{Z_{in1} + jZ_1 \tan \theta}{Z_1 + jZ_{in1} \tan \theta} \\
 &= Z_1 \frac{j \frac{\omega L_1 (\omega^2 L_2 C - 1)}{\omega^2 L_1 C + \omega^2 L_2 C - 1} + jZ_1 \tan \theta}{Z_1 - \frac{\omega L_1 (\omega^2 L_2 C - 1)}{\omega^2 L_1 C + \omega^2 L_2 C - 1} \tan \theta} \quad (4.1)
 \end{aligned}$$

To obtain an open circuit or reflection zero (RZ) at the fundamental frequency, Z_{in} must be infinite. This means that the denominator of (4.1) must equal to zero and we can determine the impedance of the RH-TL as following.

➤ Z_{in} is infinite at f_0 , so we consider ω in (4.1) is equal to ω_0 and we can write:

$$\begin{aligned}
 Z_{in} &= Z_1 \frac{j \frac{\omega_0 L_1 (\omega_0^2 L_2 C - 1)}{\omega_0^2 L_1 C + \omega_0^2 L_2 C - 1} + jZ_1 \tan \theta}{Z_1 - \frac{\omega_0 L_1 (\omega_0^2 L_2 C - 1)}{\omega_0^2 L_1 C + \omega_0^2 L_2 C - 1} \tan \theta} = \infty \\
 \Leftrightarrow Z_1 - \frac{\omega_0 L_1 (\omega_0^2 L_2 C - 1)}{\omega_0^2 L_1 C + \omega_0^2 L_2 C - 1} \tan \theta &= 0
 \end{aligned}$$

Assume : $x_1 = \omega_0^2 L_2$

$$\Rightarrow Z_1 = \frac{\omega_0 L_1 (x_1 C - 1)}{\omega_0^2 L_1 C + x_1 C - 1} \tan \theta \quad (4.2)$$

To obtain short circuit or transmission zeros (TZs) at second and third harmonic frequencies, Z_{in} must be zero. This means that the numerator of (4.1) is equal to zero and we can determine the value of L_1 and C through this condition.

- Determine for L_1 when $Z_{in} = 0$ at the third harmonic frequency ($3f_0$), so we consider ω in (4.1) is equal to $3\omega_0$ and θ is replaced by 3θ , then we can write:

$$Z_{in} = Z_1 \frac{j \frac{3\omega_0 L_1 (9\omega_0^2 L_2 C - 1)}{9\omega_0^2 L_1 C + 9\omega_0^2 L_2 C - 1} + jZ_1 \tan \theta}{Z_1 - \frac{3\omega_0 L_1 (9\omega_0^2 L_2 C - 1)}{9\omega_0^2 L_1 C + 9\omega_0^2 L_2 C - 1} \tan \theta} = 0$$

$$\text{Assume : } x_{11} = 9\omega_0^2 L_2$$

$$\Leftrightarrow \frac{3\omega_0 L_1 (x_{11} C - 1)}{9\omega_0^2 L_1 C + x_{11} C - 1} + Z_1 \tan 3\theta = 0$$

$$\Leftrightarrow \frac{3\omega_0 L_1 (x_{11} C - 1)}{9\omega_0^2 L_1 C + x_{11} C - 1} + \frac{\omega_0 L_1 (x_1 C - 1) \tan \theta \tan 3\theta}{\omega_0^2 L_1 C + x_1 C - 1} = 0$$

$$\text{Assume: } x_2 = \omega_0 \tan \theta \tan 3\theta$$

$$\Leftrightarrow \frac{3\omega_0 L_1 (x_{11} C - 1)}{9\omega_0^2 L_1 C + x_{11} C - 1} + \frac{L_1 (x_1 C - 1) x_2}{\omega_0^2 L_1 C + x_1 C - 1} = 0$$

$$\Leftrightarrow 3\omega_0 L_1 (x_{11} C - 1) (\omega_0^2 L_1 C + x_1 C - 1) + L_1 x_2 (x_1 C - 1) (9\omega_0^2 L_1 C + x_{11} C - 1) = 0$$

$$\Leftrightarrow (3\omega_0 L_1 x_{11} C - \omega_3 L_1) (\omega_0^2 L_1 C + x_1 C - 1) + (L_1 x_2 x_1 C - L_1 x_2) (9\omega_0^2 L_1 C + x_{11} C - 1) = 0$$

$$\Leftrightarrow x_{11} 3\omega_0^3 L_1^2 C^2 - 3\omega_0^3 L_1^2 C + 3\omega_0 x_1 x_{11} L_1 C^2 - 3\omega_0 x_1 L_1 C - 3\omega_0 x_{11} L_1 C + 3\omega_0 L_1 + 9\omega_0^2 x_1 x_2 L_1^2 C^2 + x_1 x_{11} x_2 L_1 C^2 - x_1 x_2 L_1 C - 9\omega_0^2 x_2 L_1^2 C - x_{11} x_2 L_1 C + x_2 L_1 = 0$$

Assume : $x_3 = 3\omega_0^3$

$$\Leftrightarrow x_{11} x_3 L_1^2 C^2 - x_3 L_1^2 C + 3\omega_0 x_1 x_{11} L_1 C^2 - 3\omega_0 L_1 C (x_1 + x_{11}) + 3\omega_0 L_1 + 9\omega_0^2 x_1 x_2 L_1^2 C^2 + x_1 x_{11} x_2 L_1 C^2 - x_2 L_1 C (x_1 + x_{11}) - 9\omega_0^2 x_2 L_1^2 C + x_2 L_1 = 0$$

$$\Leftrightarrow x_{11} x_3 L_1 C^2 - x_3 L_1 C + 3\omega_0 x_1 x_{11} C^2 - \omega_3 C (x_1 + x_{11}) + 3\omega_0 + 9\omega_0^2 x_1 x_2 L_1 C^2 + x_1 x_{11} x_2 C^2 - x_2 C (x_1 + x_{11}) - 9\omega_0^2 x_2 L_1 C + x_2 = 0$$

$$\Leftrightarrow L_1 (x_{11} x_3 C^2 - x_3 C + 9\omega_0^2 x_1 x_2 C^2 - 9\omega_0^2 x_2 C) = 3\omega_0 C (x_1 + x_{11}) - 3\omega_0 x_1 x_{11} C^2 - 3\omega_0 - x_1 x_{11} x_2 C^2 + x_2 C (x_1 + x_{11}) - x_2$$

$$\Rightarrow L_1 = \frac{3\omega_0 C (x_1 + x_{11}) - 3\omega_0 x_1 x_{11} C^2 - 3\omega_0 - x_1 x_{11} x_2 C^2 + x_2 C (x_1 + x_{11}) - x_2}{(x_{11} x_3 + 9\omega_0^2 x_1 x_2) C^2 - (x_3 + 9\omega_0^2 x_2) C}$$

$$= \frac{C (x_1 + x_{11}) (3\omega_0 + x_2) - (3\omega_0 + x_2) x_1 x_{11} C^2 - (3\omega_0 + x_2)}{(x_{11} x_3 + 9\omega_0^2 x_1 x_2) C^2 - (x_3 + 9\omega_0^2 x_2) C} \quad (4.3a)$$

$$= \frac{[(x_1 + x_{11}) C - x_1 x_{11} C^2 - 1] (3\omega_0 + x_2)}{(x_{11} C - 1) (x_3 C + 9\omega_0^2 x_2 C)} \quad (4.3b)$$

- Determine C when $Z_{in} = 0$ at the second harmonic frequency ($2f_0$), so we consider ω in (4.1) is equal to $2\omega_0$ and θ is replaced by 2θ , then we can write:

$$Z_{in} = Z_1 \frac{j \frac{2\omega_0 L_1 (4\omega_0^2 L_2 C - 1)}{4\omega_0^2 L_1 C + 4\omega_0^2 L_2 C - 1} + jZ_1 \tan 2\theta}{Z_1 - \frac{2\omega_0 L_1 (4\omega_0^2 L_2 C - 1)}{4\omega_0^2 L_1 C + 4\omega_0^2 L_2 C - 1} \tan 2\theta} = 0$$

$$\Leftrightarrow \frac{2\omega_0 L_1 (4\omega_0^2 L_2 C - 1)}{4\omega_0^2 L_1 C + 4\omega_0^2 L_2 C - 1} + Z_1 \tan 2\theta = 0$$

$$\text{Assume : } x_{12} = 4\omega_0^2 L_2$$

$$\Leftrightarrow \frac{2\omega_0 L_1 (x_{12} C - 1)}{4\omega_0^2 L_1 C + x_{12} C - 1} + Z_1 \tan 2\theta = 0$$

$$\Leftrightarrow 2\omega_0 x_{12} L_1 C - 2\omega_0 L_1 + 4\omega_0^2 Z_1 L_1 C \tan 2\theta + Z_1 x_{12} C \tan 2\theta - Z_1 \tan 2\theta = 0 \quad (4.4)$$

From (4.3a)

$$L_1 = \frac{C(x_1 + x_{11})(2\omega_0 + x_2) - (3\omega_0 + x_2)x_1 x_{11} C^2 - (3\omega_0 + x_2)}{(x_1 x_3 + 9x_1 x_2 \omega_0^2) C^2 - (x_3 + 9x_2 \omega_0^2) C}$$

From (2)

$$Z_1 = \frac{\omega_0 L_1 (x_1 C - 1)}{\omega_0^2 L_1 C + x_1 C - 1} \tan \theta = \frac{\omega_0 L_1 \tan \theta x_1 C - \omega_0 L_1 \tan \theta}{\omega_0^2 L_1 C + x_1 C - 1}$$

$$\text{Assume : } a_1 = (x_1 + x_{11})(3\omega_0 + x_2)$$

$$a_2 = (3\omega_0 + x_2)x_1 x_{11}$$

$$a_3 = 3\omega_0 + x_2$$

$$a_4 = x_{11} x_3 + 9x_1 x_2 \omega_0^2$$

$$a_5 = x_3 + 9x_2 \omega_0^2$$

$$a_6 = \omega_0 \tan \theta$$

We can write:

$$L_1 = \frac{a_1 C - a_2 C^2 - a_3}{a_4 C^2 - a_5 C} \quad (4.5)$$

$$Z_1 = \frac{a_6 x_1 L_1 C - L_1 a_6}{\omega_0^2 L_1 C + x_1 C - 1} = \frac{L_1 (a_6 x_1 C - a_6)}{\omega_0^2 L_1 C + x_1 C - 1} \quad (4.6)$$

Substitute (4.6) to (4.4):

$$\begin{aligned} \Leftrightarrow & 2x_{12}\omega_0 L_1 C - 2\omega_0 L_1 + \frac{L_1 (a_6 x_1 C - a_6)}{\omega_0^2 L_1 C + x_1 C - 1} 4\omega_0^2 L_1 C \tan 2\theta \\ & + \frac{L_1 (a_6 x_1 C - a_6)}{\omega_0^2 L_1 C + x_1 C - 1} x_{12} C \tan 2\theta - \frac{L_1 (a_6 x_1 C - a_6)}{\omega_0^2 L_1 C + x_1 C - 1} \tan 2\theta = 0 \end{aligned}$$

Divide equation with L_1 :

$$\begin{aligned} \Leftrightarrow & 2x_{12}\omega_0 C - 2\omega_0 + \frac{(a_6 x_1 C - a_6)}{\omega_0^2 L_1 C + x_1 C - 1} 4\omega_0^2 L_1 C \tan 2\theta \\ & + \frac{(a_6 x_1 C - a_6)}{\omega_0^2 L_1 C + x_1 C - 1} x_{12} C \tan 2\theta - \frac{(a_6 x_1 C - a_6)}{\omega_0^2 L_1 C + x_1 C - 1} \tan 2\theta = 0 \end{aligned}$$

$$\begin{aligned} \Leftrightarrow & 2x_{12}\omega_0 C (\omega_0^2 L_1 C + x_1 C - 1) - 2\omega_0 (\omega_0^2 L_1 C + x_1 C - 1) \\ & + (a_6 x_1 C - a_6) 4\omega_0^2 L_1 C \tan 2\theta + (a_6 x_1 C - a_6) x_{12} C \tan 2\theta \\ & - (a_6 x_1 C - a_6) \tan 2\theta = 0 \end{aligned}$$

$$\begin{aligned} \Leftrightarrow & 2x_{12}\omega_0^3 L_1 C^2 + 2x_{12}\omega_0 x_1 C^2 - 2x_{12}\omega_0 C - 2\omega_0^3 L_1 C - 2\omega_0 x_1 C \\ & + 2\omega_0 + 4a_6 x_1 \omega_0^2 L_1 C^2 \tan 2\theta - 4a_6 \omega_0^2 L_1 C \tan 2\theta + 4a_6 x_1 x_{12} \omega_0^2 C^2 \tan 2\theta \\ & - a_6 x_{12} C^2 \tan 2\theta - a_6 x_1 C \tan 2\theta + a_6 \tan 2\theta = 0 \end{aligned}$$

Assume : $b_1 = 2\omega_0^3$

$$b_2 = 2x_{12}\omega_0x_1$$

$$b_3 = 2\omega_0(x_1 + x_{12})$$

$$b_4 = 4a_6\omega_0^2 \tan 2\theta$$

$$b_5 = a_6x_{12} \tan 2\theta$$

$$b_6 = a_6 \tan 2\theta$$

We can write:

$$\begin{aligned} x_{12}b_1L_1C^2 + b_2C^2 - b_3C - b_1L_1C + 2\omega_0 + b_4x_1L_1C^2 \\ - b_4L_1C + b_5x_1C^2 - b_5C - b_6x_1C + b_6 = 0 \end{aligned}$$

$$\Leftrightarrow (x_{12}b_1C + b_4x_1C - b_1 - b_4)CL_1 = b_3C - b_2C^2 - 2\omega_0 \\ - b_5x_1C^2 + b_5C + b_6x_1C - b_6$$

$$\Leftrightarrow (x_{12}b_1C + b_4x_1C - b_1 - b_4)C \left(\frac{a_1C - a_2C^2 - a_3}{a_4C^2 - a_5C} \right) = b_3C - b_2C^2 - 2\omega_0 \\ - b_5x_1C^2 + b_5C + b_6x_1C - b_6$$

$$\Leftrightarrow ((x_{12}b_1 + b_4x_1)C - (b_1 + b_4)) \left(\frac{a_1C - a_2C^2 - a_3}{a_4C - a_5} \right) = (b_3 + b_5 + b_6x_1)C \\ - (b_2 + b_5x_1)C^2 - (2\omega_0 + b_6)$$

Assume : $E_1 = b_3 + b_5 + b_6x_1$

$$E_2 = 2\omega_0 + b_6$$

$$E_3 = x_{12}b_1 + b_4x_1$$

$$E_4 = b_1 + b_4$$

$$E_5 = b_2 + b_5x_1$$

$$\Leftrightarrow (E_3C - E_4)(a_1C - a_2C^2 - a_3) = (a_4C - a_5)(E_1C - E_5C^2 - E_2)$$

$$\Leftrightarrow C^3(a_4E_2 - E_3a_2) + C^2(E_3a_1 + E_4a_2 - E_1a_4 - E_2a_5) \\ - C(E_3a_3 + E_4a_1 - a_5E_1 - a_4E_2) + E_4a_3 - a_5E_2 = 0 \quad (4.7)$$

According to the derived equation, we can use (4.7), (4.3b), and (4.2) to solve for C , L_1 , and Z_1 , respectively. We can obtain the value of the elements in the biasing circuit using CRLH TL as the following flowchart.

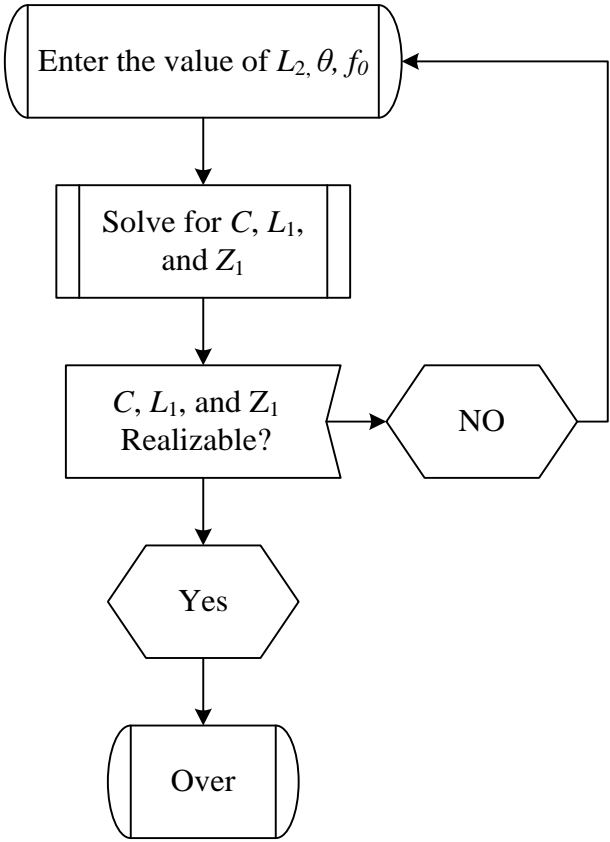


Fig. 4.4. The flowing chart to optimize the value of the elements in CRLH bias circuit.

4.1.3 Analysis of an Impedance Transformer Using CRLH TL

Now we can obtain a reflection zero (open circuit) for fundamental and two transmission zero (short circuit) for second and third harmonic frequencies at the connection point of the circuit in Fig. 4.2, but we still have to consider how to obtain short circuit for the second harmonic and open circuit for the third harmonic at the drain terminal of the transistor. Most of the previous works, the quarter wavelength transmission line are presented to obtain this condition [9]. As a result, the overall size of the circuit is increased. In this work, we use the CRLH structure instead of the quarter wavelength transmission line. Our target is to obtain short ($2f_0$) and open ($3f_0$) circuits at the drain terminal of the transistor by transforming the impedance at the connection point in Fig. 4.2. We can obtain this condition by the following analysis. Fig. 4.4 shows the proposed structure that will take the place of quarter wavelength transmission line.

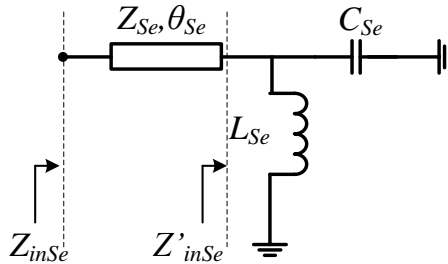


Fig. 4.4. The structure of the impedance transformer circuit.

We use the same analysis method in the above section to fulfill the requirement of class-F PAs. The subscript Se , representation the series connection of the structure when applying to PA design.

➤ Determine Z_{inSe}

$$Z'_{inSe} = \frac{j\omega L_{Se} \times \frac{1}{j\omega C_{Se}}}{j\omega L_{Se} + \frac{1}{j\omega C_{Se}}} = \frac{j\omega L_{Se}}{1 - \omega^2 L_{Se} C_{Se}}$$

$$Z_{inSe} = Z_{Se} \frac{Z'_{inSe} + jZ_{Se} \tan \theta_{Se}}{Z_{Se} + jZ'_{inSe} \tan \theta_{Se}}$$

$$= Z_{Se} \frac{j \frac{\omega L_{Se}}{1 - \omega^2 L_{Se} C_{Se}} + jZ_{Se} \tan \theta_{Se}}{Z_{Se} - \frac{\omega L_{Se}}{1 - \omega^2 L_{Se} C_{Se}} \tan \theta_{Se}} \quad (4.8)$$

➤ Determine Z_{Se} when $Z_{inSe} = \infty$ at the third harmonic frequency ($3f_0$).

The ratio of $3f_0/2f_0$ is 1.5, so we consider ω in (4.8) is equal to $1.5\omega_2$ and θ_{Se} is replaced $1.5\theta_{Se}$, where $\omega_2 = 2\omega_0$, θ_{Se} is the electrical length of RH TL at $2f_0$. For $Z_{inSe} = \infty$, the denominator of (4.8) must be equal to zero.

$$Z_{Se} - \frac{1.5\omega_2 L_{Se}}{1 - (1.5\omega_2)^2 L_{Se} C_{Se}} \tan 1.5\theta_{Se} = 0$$

$$\Rightarrow Z_{Se} = \frac{1.5\omega_2 L_{Se}}{1 - (1.5\omega_2)^2 L_{Se} C_{Se}} \tan 1.5\theta_{Se}$$

$$= \frac{1.5 \times 2\omega_0 L_{Se}}{1 - (1.5 \times 2\omega_0)^2 L_{Se} C_{Se}} \tan 1.5\theta_{Se}$$

$$= \frac{3\omega_0 L_{Se}}{1 - 9\omega_0^2 L_{Se} C_{Se}} \tan 1.5\theta_{Se} \quad (4.8)$$

- Determine Z_{Se} when $Z_{inSe} = 0$ at second harmonic frequency ($2f_0$). We consider ω in (4.8) is equal to ω_2 , where $\omega_2 = 2\omega_0$, θ_{Se} is the electrical length of RH TL at $2f_0$. For $Z_{inSe} = 0$, the numerator of (4.8) must be equal to zero.

$$\Leftrightarrow \frac{\omega_2 L_{Se}}{1 - \omega_2^2 L_{Se} C_{Se}} + Z_{Se} \tan \theta_{Se} = 0$$

$$\Leftrightarrow \frac{\omega_2 L_{Se}}{1 - \omega_2^2 L_{Se} C_{Se}} + \frac{3\omega_0 L_{Se}}{1 - 9\omega_0^2 L_{Se} C_{Se}} \tan 1.5\theta_{Se} \tan \theta_{Se} = 0$$

$$\text{Assume : } P = 3\omega_0 L_{Se} \tan 1.5\theta_{Se} \tan \theta_{Se}$$

$$\Leftrightarrow \omega_2 (1 - 9\omega_0^2 L_{Se} C_{Se}) + P(1 - \omega_2^2 L_{Se} C_{Se}) = 0$$

$$\Leftrightarrow \omega_2 - 9\omega_2 \omega_0^2 L_{Se} C_{Se} + P - P\omega_2^2 L_{Se} C_{Se} = 0$$

$$\Leftrightarrow \omega_2 + P = (9\omega_2 \omega_0^2 L_{Se} + P\omega_2^2 L_{Se}) C_{Se}$$

$$\Rightarrow C_{Se} = \frac{\omega_2 + P}{9\omega_2 \omega_0^2 L_{Se} + P\omega_2^2 L_{Se}}$$

$$= \frac{2\omega_0 + P}{18\omega_0^3 L_{Se} + 4P\omega_0^2 L_{Se}} \quad (4.9)$$

According to the derived equation, we can use (4.8), and (4.9) to solve for C_{Se} , and Z_{Se} , respectively, where L_{Se} and θ_{Se} are assumed. We can obtain the value of the elements in the harmonic impedance transformer circuit with the same process to the flow chart in Fig. 4.4.

4.2 Class-F Power Amplifier Design

This section presents the design procedure of class-F PA using harmonic control CRLH TL.

4.2.1 Load-pull method

For many years, the exact value of power impedance at RF and microwave frequencies was regarded as something that could be measured only experimentally. Thus, the art and science of Load-pull are provided in a computer-controlled system, the complexity of the procedure to find the optimum impedances for PAs design are reduced. Microwave simulation software ADS has load-pull and source-pull control simulation tools. Large signal model of the transistor can be imported into ADS to process load-pull and source-pull to select the optimum source and load impedances. Load-pull data has been the mainstay of RF and microwave PA design for many years. It gives the designer a simple target area on the Smith chart on which to base the strategy for suitable matching network design. The simulation model of CGH40010F GaN HEMT provided by Wolfspeed is used in this design. The bias condition were $V_{DD} = 25$ V, $V_{GS} = -2.75$ V, and $I_{dq} = 202$ mA at. The optimum load impedance is $Z_L = 15.66 + j13.76 \Omega$ and optimum source impedance is $Z_S = 17.53 - j11.42 \Omega$. In this design, the impedance of the second and third harmonics are assumed as short and open, respectively.

Fig. 4.5 shows the procedure to obtain the load impedance for output matching network design. After we import the CRLH TLs structure of bias circuit and impedance transformer to the load-pull simulation, the load

impedance is transformed to $110.48 + j77.12 \Omega$. The contours of PAE and power delivered to the load is presented in Fig. 4.6.

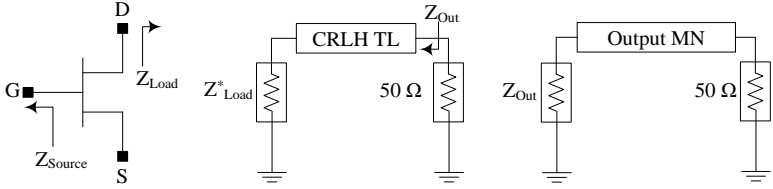


Fig. 4.5. The procedure to obtain the impedance to the output matching network.

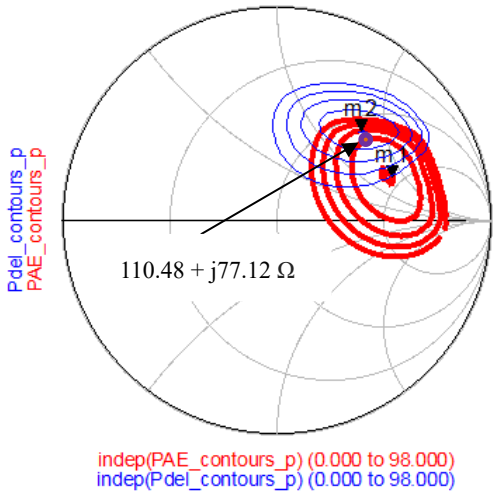


Fig. 4.6. Contours of PAE and power delivered to the load obtain from load-pull simulation.

4.2.2 Biasing Circuit Design

In this work, the bias circuit is designed by using CRLH TL. The purpose of using this CRLH TL structure is to reduce the size of the bias circuit and it also can provide open circuit at f_0 , short circuit at $2f_0$ and $3f_0$. Generally, the quarter wavelength ($\lambda/4$) TL used for bias line can obtain open circuit at f_0 , short circuit at $2f_0$ and open circuit at $3f_0$. According to this result, the harmonic control circuit is added to PA design in class-F. In this work, we can control the harmonic components to fulfill the class-F PA requirement easily by using impedance transformer TL. The structure of the bias circuit using CRLH TL is presented in Fig. 4.7. The DC is feed from the inductor L_1 . A shunt capacitor is connected to the DC feed point for RF-short.

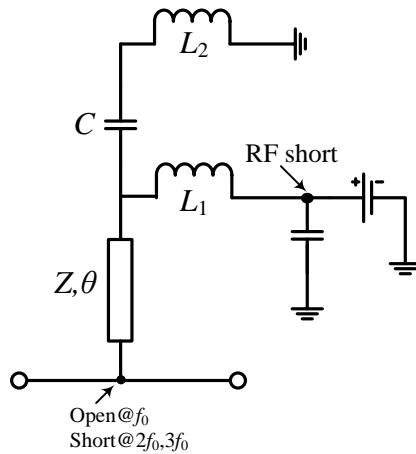


Fig. 4.7. Biasing circuit with harmonic control using CRLH TL.

Using (4.7), (4.3b), and (4.2) to solve for C , L_1 and the impedance of microstrip line (MSL), when the electrical length of MSL is 58° and $L_2 = 7.4$ nH. As the result the impedance of MSL is 79.11Ω , $L_1 = 3.75$ nH and $C = 0.1$ pF. Fig. 4.8 shows the simulation results of the biasing circuit using CRLH TL.

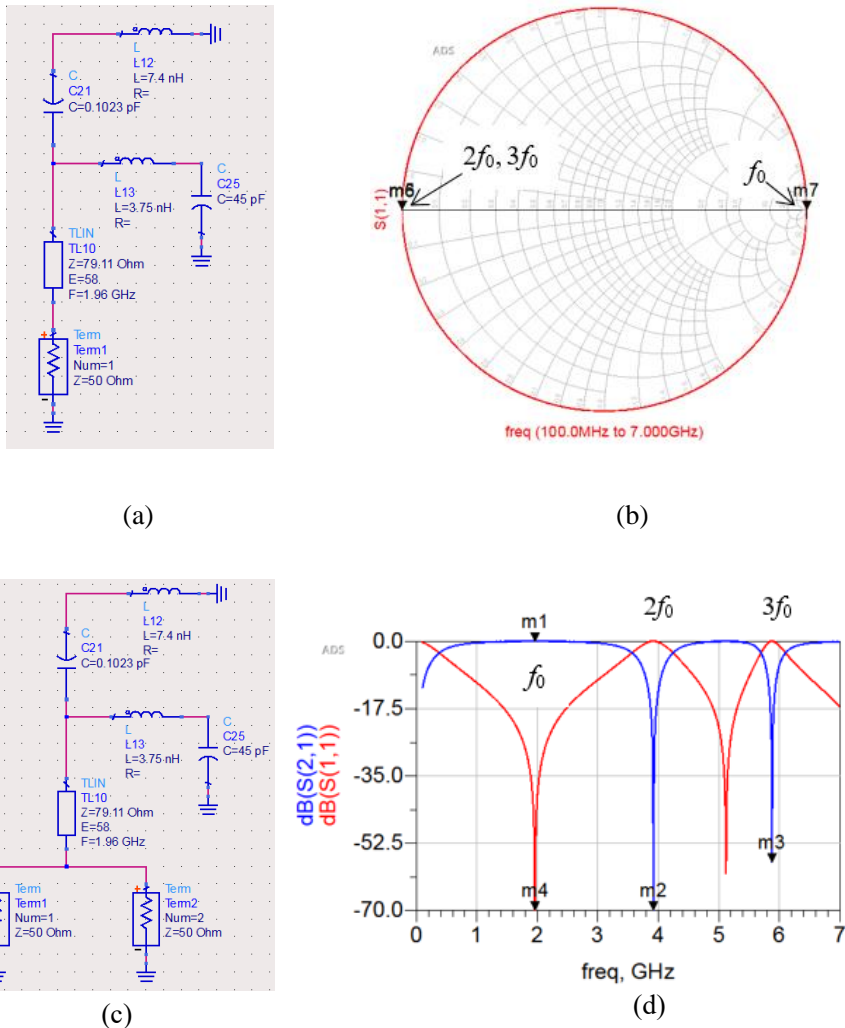


Fig. 4.8. Bias circuit: (a) one-port network, (b) impedances point, (c) two-ports network, and (d) S -parameters.

4.2.3 Impedance Transformer

In this work, we don't use $\lambda/4$ TL to transform the impedance at the connection point of the biasing circuit. To obtain the short circuit for $2f_0$ and open circuit for $3f_0$ at the drain terminal of the transistor we use the structure in Fig. 4.5 and its analysis in section 4.1.3. Fig. 4.9 shows the impedance transforming structure.

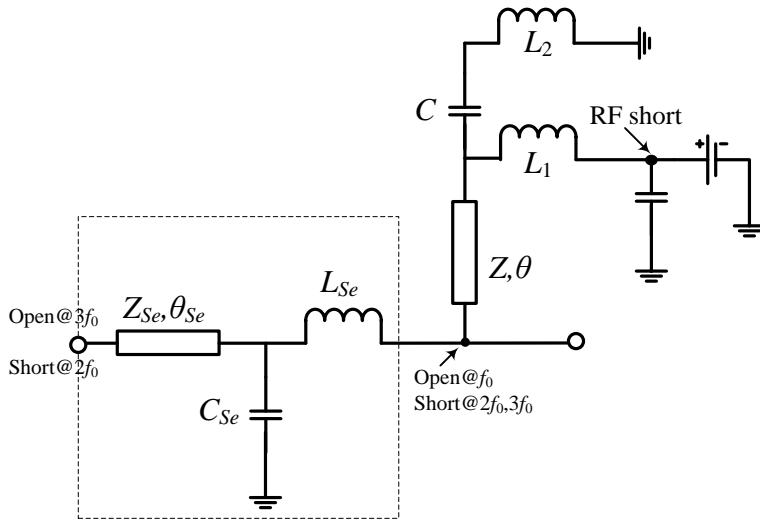
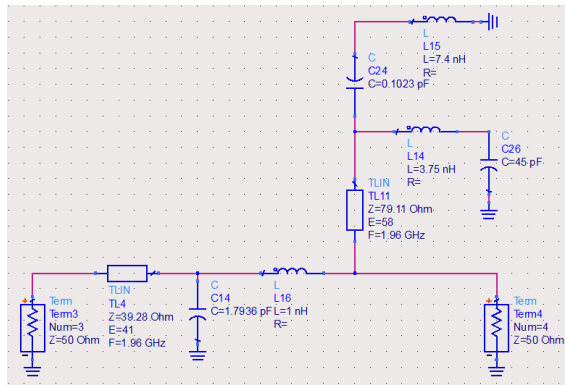
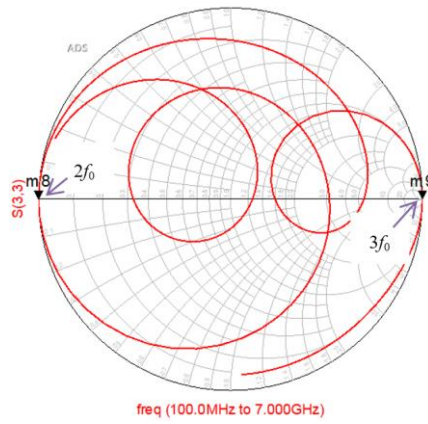


Fig. 4.9. Impedance transforming structure.

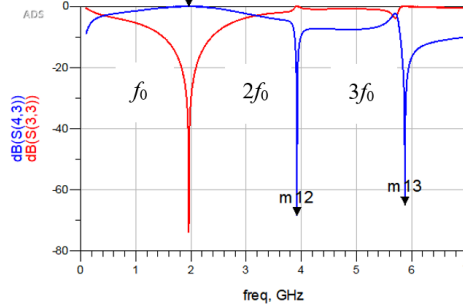
Using (4.8) and (4.9) to solve for Z_{Se} and C_{Se} , when the electrical length of TL, $\theta_{Se} = 41^\circ$ and $L_{Se} = 1$ nH. As a result, the impedance of $Z_{Se} = 39.24 \Omega$, and $C_{Se} = 1.79$ pF. Fig. 4.10 shows the simulation results of the impedance transforming circuit.



(a)



(b)



(c)

Fig. 4.10. Impedance transformer: (a) simulated circuit, (b) impedance points and (c) S -parameters.

4.2.4 Matching Networks Design

Impedance matching is very important in PAs design. In conventional PA design, the output matching network (OMN) is normally choose the impedances at the point of the maximum power or maximum power added efficiency (PAE) depending on the load-pull process. As shown in Fig. 4.11, PA is modeled as a two-port network. Γ_S is the reflection coefficient seen from the output port of the input matching network toward the generator. Γ_L is the reflection coefficient seen from the input port of the output matching network toward the load. Γ_{opt-in} is the optimum reflection coefficient seen from the gate terminal of the transistor when the drain terminal is terminated with an output matching network. $\Gamma_{opt-out}$ is the optimum reflection coefficient seen from the drain terminal when the gate terminal is terminated with an input matching network. The input and output matching networks are designed to match the optimum impedances at the gate and drain terminal for maximum output power and efficiency.

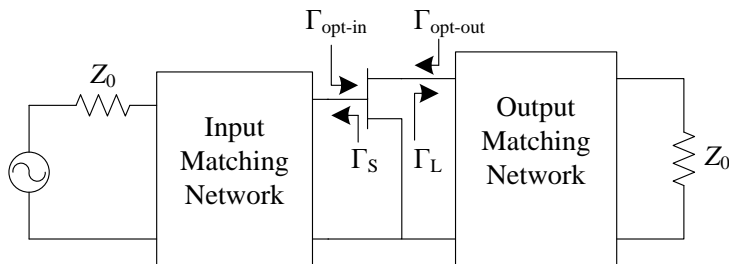


Fig. 4.11. PAs design and impedance matching.

Fig. 4.12 shows the equivalent circuit of class-F PA in this work. CRLH TL biasing circuits are applied to input and output parts. Stability and oscillation suppression are important factors to be considered in amplifier design. The parallel of $10\ \Omega$ resistor with a $0.74\ \text{pF}$ capacitor followed by $47\ \Omega$ resistor at the gate bias line are worked as amplifier stabilizer. This stability circuit obtained the stability factor larger than 1. The input matching network (IMN) and output matching network (OMN) are designed with lump elements. These lumped elements in the circuit will realize to the transmission lines.

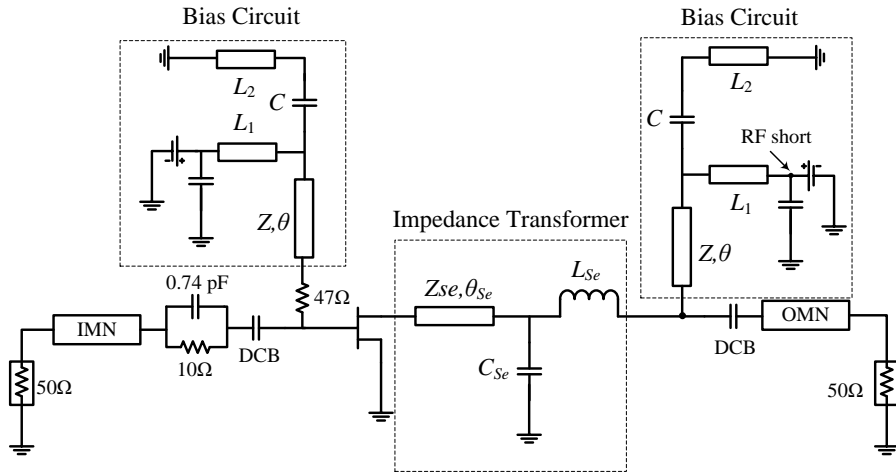


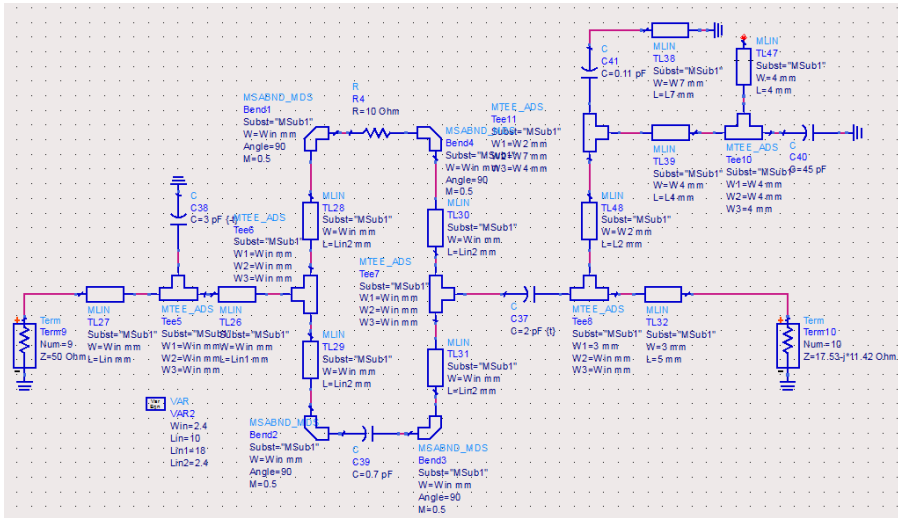
Fig. 4.12. The equivalent circuit of class-F PA with harmonic control using CRLH TLs.

In [13], the equivalent value of lumped elements to the transmission line is presented below.

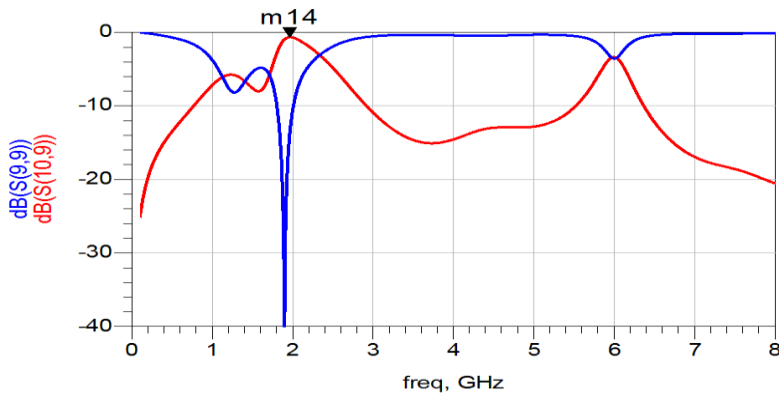
$$L_t = \frac{Z_t \sin \theta}{\omega} \quad (4.1)$$

$$C_t = \frac{1 - \cos \theta}{Z_t \omega \sin \theta} \quad (4.2)$$

Fig. 4.13 and Fig. 4.14 show the input and output circuit of the designed class-F PA. The input circuit is constructed by IMN, stability circuit, DC-block and bias circuit to the gate terminal of the transistor.



(a)

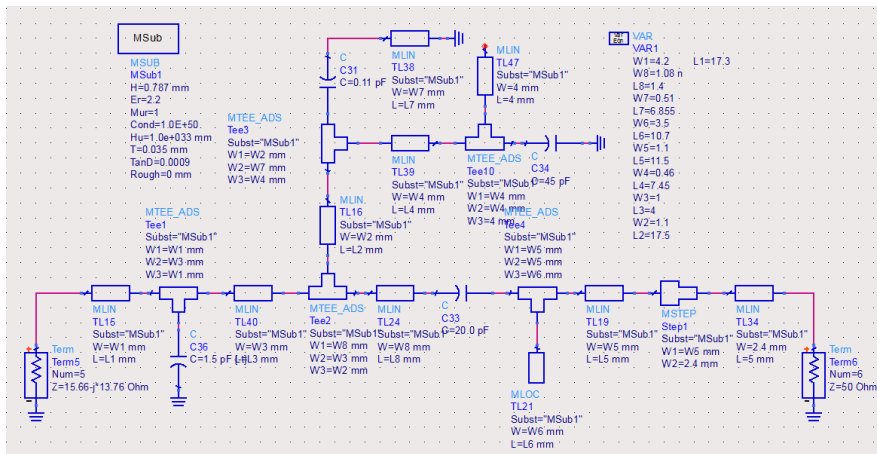


(b)

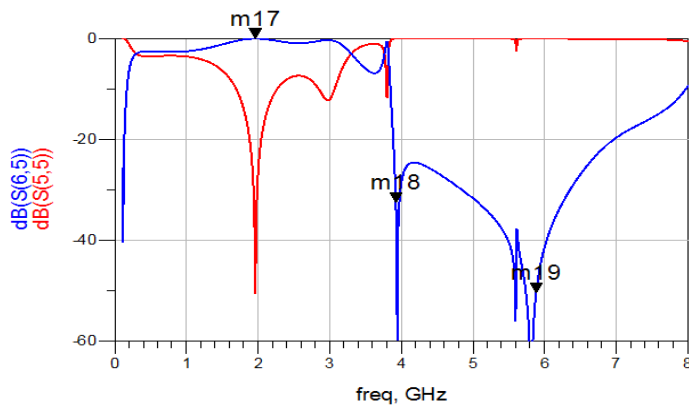
Fig. 4.13. Input circuit: (a) input matching network with stability and bias circuits and (b) S -parameters.

The output circuit is constructed by harmonic impedance transformer circuit, drain bias circuit, DC-block, and OMN to the 50Ω load. According to

the parasitics components within the package of the transistor, the length of the impedance transformer TL is required more than $\lambda/4$ to obtain short circuit at $2f_0$ and open circuit at $3f_0$. In this work, our harmonic impedance transformer circuit has a relation to CRLH TL and it can obtain these requirements with the overall length smaller than $\lambda/4$. The IMN and OMN of PA are designed on RT/Duriod 5880 substrate from Roger Inc., with a dielectric constant (ϵ_r) of 2.2 and thickness (h) of 31 mils.



(a)



(b)

Fig. 4.14. Output circuit: (a) harmonic control circuit with matching network and (b) S-parameters.

4.2.5 Simulation results

In this section, the simulation results of class-F PA are presented. The bias condition $V_{DD} = 25$ V, $V_{GS} = -2.75$ V, and $I_{dq} = 202$ mA. Fig. 4.16 shows the S -parameters of the simulated PA. The magnitude at f_0 of S_{21} , S_{11} , and S_{22} are 14.31 dB, -6.55 dB, and -11 dB, respectively. Fig. 4.17 shows the performances of the PA. The output power, drain efficiency and PAE are 13.61 W, 70.39% and 66.63% at center frequency 1.96 GHz.

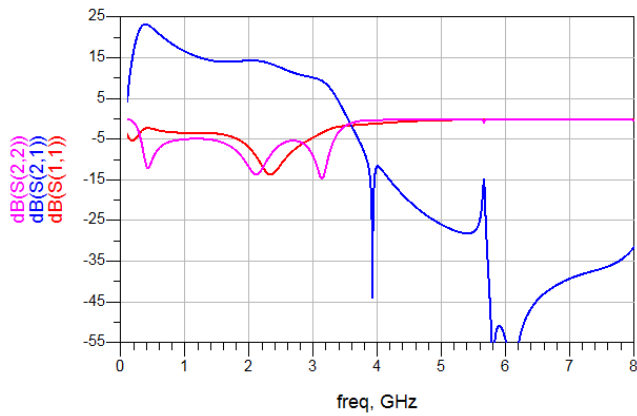


Fig. 4.15. S -parameters of class-F PA.

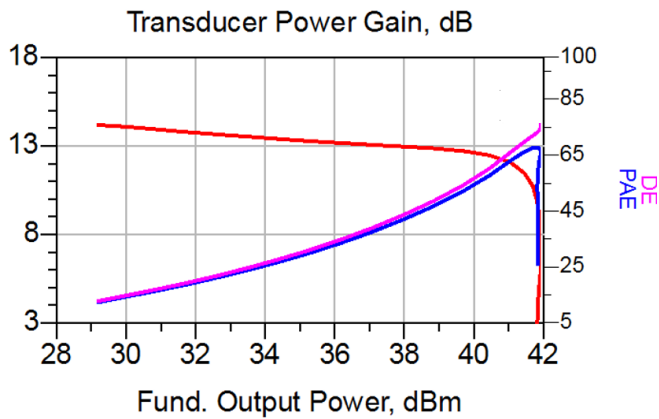


Fig. 4.16. Gain, drain efficiency and PAE along the output power.

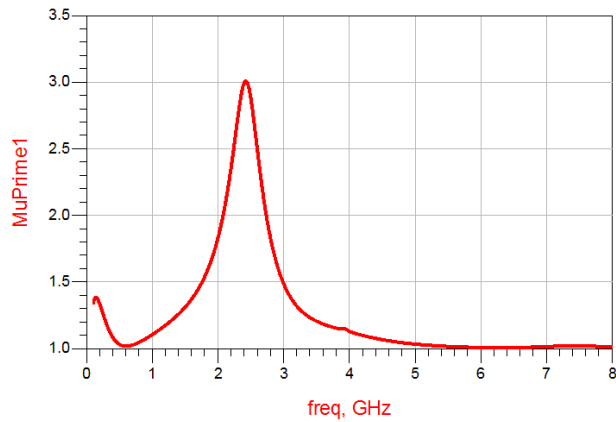


Fig. 4.17. Stability factor of the simulated PA.

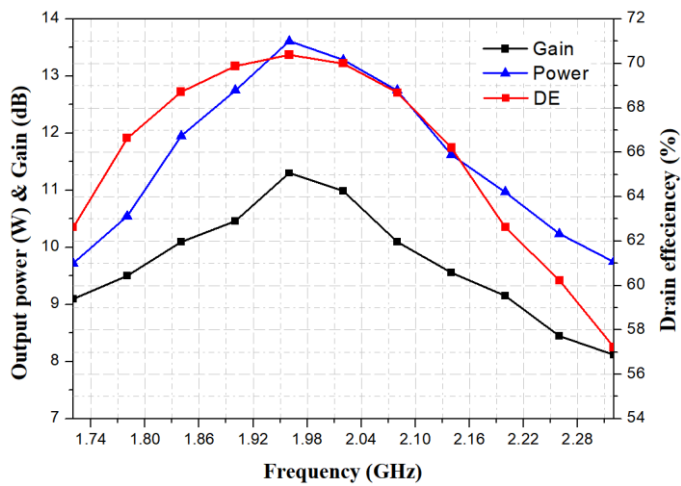


Fig. 4.18. Output power, gain, and drain efficiency along the frequencies.

Fig. 4.18 presents the stability factor of the designed PA. As a result, the Mu-factor is greater than 1 at all any frequency and it confirms that the stability circuit can suppress the oscillation. Fig. 4.19 present the performance of the designed PA along the frequencies.

As the results in Fig. 4.19, the designed PA provided the similar performance when it operates in PCS downlink-band. The saturation gain, drain efficiency, and output power are dropped at lower and upper PCS band.

In this section, the design method and analysis is done and confirmed by the simulation. A class-F PA for PCS downlink frequency band operation provide output power more than 10 W.

Chapter 5 Conclusions and Future Work

A microwave class-F power amplifier using the harmonic control CRLH transmission line is designed in this thesis. The mathematical analysis of the harmonic control circuit is provided. The biasing circuit has the ability to control up to the third harmonic at the exact frequency position. The length of the TL in the biasing circuit is smaller than $\lambda/4$. According to the parasitic components within the transistor package, it required more than $\lambda/4$ TL to obtain short and open circuit for second and third harmonic frequencies, respectively, but to obtain this requirement, the proposed impedance transformer required less than $\lambda/4$ of TL. The output power, drain efficiency and PAE of the designed PA are 13.61 W, 70.39% and 66.63% at center frequency 1.96 GHz. It provides almost the same performance when operate in whole of PCS downlink frequency band from 1.93 GHz to 1.99 GHz.

Taking advantages of the unique property of CRLH TL, these proposed circuits should be able to use in wider application.

References

- [1] G. Nikandish, E. Babakrpur, A. Medi, "Harmonic Termination Technique for Single- and Multi-Band High-Efficiency Class-F MMIC Power Amplifiers", *IEEE Trans. Microw. Theory & Tech.*, vol. 62, no. 5, May 2014.
- [2] K. Chen, and D. Peroulis, "Design of broadband highly efficient harmonic-tuned power amplifier using in-band continuous class-F¹/F mode transferring", *IEEE Trans. Microw. Theory & Tech.*, vol. 60, no. 12, pp. 4107-4116, December 2012.
- [3] Seth W. Waldstein, Miguel A. Barbosa Kortright, Rainee N. Simons, "Multiband Reconfigurable Harmonically Tuned GaN SSPA for Cognitive Radios," in *NASA/TM*, 2017, pp. 1–7.
- [4] S. C. Cripps, *RF Power Amplifier for Wireless Communication*, Second edition, Artech House Publishers, 2006.
- [5] Y. Jeong, G. Chaudhary, J. Lim, "A Dual Band High Efficiency Class-F GaN Power Amplifier Using Harmonic Rejection Load Network", *IEICE Trans. Electron.*, vol. E95-C, no. 11, November 2012.
- [6] Q. Wang, J. Lim, Y. Jeong, "Design of a compact dual-band branch line coupler using composite right/left-handed transmission lines", *Electronics Letters.*, vol. 52, no. 8, pp. 630-631, April 2016.
- [7] C. Caloz and T. Itoh, *Electromagnetic Metamaterials, TransmissionLine Theory and Microwave Applications*, New York: Wiley, 2005.

- [8] D.M. Pozar, *Microwave engineering*, Wiley, New York, 1998.
- [9] S. Tanaka, T. Oda, K. Saiki, “ Novel DC-Bias Circuit with Arbitrary Harmonic-Control Capability for Compact High-Efficiency Power Amplifiers”, *48th European Microwave Conference*, September 2018.
- [10] S. Tanaka, K. Muhaida, K. Takata, “ Compact Stub Resonators with Enhanced Q-Factor Using Negative Order Resonance Modes of Non-Uniform CRLH Transmission Lines”, *IEICE Trans. Electron.*, vol. E98-C, no. 3, March 2015.
- [11] S. Tanaka, S. Koizumi and K. Saito, "Compact harmonic tuning circuits for class-F amplifiers using negative order resonance modes of CRLH stub lines," in *46th European Microwave Conference*, pp. 1063-1066, 2016.
- [12] S. Tanaka, K. Saito, T. Oka, and Y. Shibosawa, “Applications of dispersion-engineered composite right-/left-handed transmission line stubs for microwave active circuits,” *IEICE Trans. Electron.*, vol. E100-C, no. 10, pp. 866-874, 2017.
- [13] S. Park, H. Choi, Y. Jeong, “Microwave Group Delay Time Adjuster Using Parallel Resonator”, *IEEE Microw. & Wireless Component Letts.*, vol. 17, no. 2, February 2007.

요약

이 논문은 CRLH (composite right/left handed) 전송선로를 이용한 고조파 제어 마이크로파 F 급 전력증폭기 연구를 제시한다. 제안하는 전력 증폭기는 사이즈를 줄이기 위해 비대칭/비균형 CRLH 전송선로를 이용해 바이어스 회로 및 임피던스 변환기를 구현했다. 이 CRLH TL 은 고조파 제어 목적으로 바이어스 회로 설계에 적용된다. 제안된 바이어스 회로에서 TL 의 길이는 $\lambda/4$ 보다 작다. $\lambda/4$ TL 을 사용하는 대신 임피던스 변환기를 CRLH TL 로 분석하여 트랜지스터의 드레인 단자에서 각각 $2f_0$ 및 $3f_0$ 에 대한 단락 및 개방 회로를 얻는다. 결과적으로 제안된 임피던스 변환기 회로는 TL 의 전기 길이가 90° 미만인 요구 사항을 만족할 수 있다.

제안 회로의 특성을 검증하기 위해 1.96 GHz personal communication services (PCS) 하향 대역에서 CRLH 전송선로를 이용한 고조파 제어 마이크로파 F 급 전력증폭기를 설계 했다. 설계 결과 제안하는 전력증폭기는 13.61 W 및 70.39%의 출력 전력 및 드레인 효율을 얻었다.

주요어: CRLH TL, 고조파, 전력증폭기, PCS.